

JAERI-Review
2005-024
(RT/2005/2/MAT(ENEA))



JP0550294



Li DEPLETION EFFECTS ON Li_2TiO_3 REACTION WITH H_2
IN THERMO-CHEMICAL ENVIRONMENT
RELEVANT TO BREEDING BLANKET FOR FUSION POWER PLANTS

REPORT OF WORKING GROUP (TASK F AND WG-F) IN THE SUBTASK ON SOLID BREEDER BLANKETS
UNDER IEA CO-OPERATIVE PROGRAMME ON NUCLEAR TECHNOLOGY OF FUSION REACTORS

July 2005

Carlo ALVANI*, Sergio CASADIO*, Vittoria CONTINI*, Rossella GIORGI*,
Maria Rita MANCINI*, Kunihiko TSUCHIYA and Hiroshi KAWAMURA

日本原子力研究所
Japan Atomic Energy Research Institute

本レポートは、日本原子力研究所が不定期に公刊している研究報告書です。

入手の問合せは、日本原子力研究所研究情報部研究情報課（〒319-1195 茨城県那珂郡東海村）あて、お申し越し下さい。なお、このほかに財団法人原子力弘済会資料センター（〒319-1195 茨城県那珂郡東海村日本原子力研究所内）で複写による実費頒布をおこなっております。

This report is issued irregularly.

Inquiries about availability of the reports should be addressed to Research Information Division, Department of Intellectual Resources, Japan Atomic Energy Research Institute, Tokai-mura, Naka-gun, Ibaraki-ken, 319-1195, Japan.

© Japan Atomic Energy Research Institute, 2005

編集兼発行 日本原子力研究所

© Ente per le Nuove tecnologie, l'Energia e l'Ambiente, 2005

Li Depletion Effects on Li_2TiO_3 Reaction with H_2 in Thermo-chemical Environment Relevant to Breeding Blanket for Fusion Power Plants

Carlo ALVANI*, Sergio CASADIO*, Vittoria CONTINI*, Rossella GIORGI*,
Maria Rita MANCINI*, Kunihiro TSUCHIYA and Hiroshi KAWAMURA

Department of Fusion Engineering Research
(Oarai Site)
Naka Fusion Research Establishment
Japan Atomic Energy Research Institute
Oarai-machi, Higashibaraki-gun, Ibaraki-ken

(Received May 16, 2005)

This is a report of the Working Group in the Subtask on Solid Breeder Blankets under the Implementing Agreement on a Co-operative Programme on Nuclear Technology of Fusion Reactors (International Energy Agency (IEA)). This Working Group (Task F and WG-F) was performed from 2000 to 2004 by a collaboration of European Union (EU) and Japan (JA). In this report, lithium depletion effects on the reaction of lithium titanate (Li_2TiO_3) with hydrogen (H_2) in thermo-chemical environment were discussed.

The reaction of Li_2TiO_3 ceramics with H_2 was studied in a thermo-chemical environment simulating (excepting irradiation) that of the hottest pebble-bed zone of breeding-blanket actually designed for fusion power plants. This “reduction” as performed at 900°C in $\text{Ar}+0.1\%\text{H}_2$ purge gas ($\text{He}+0.1\%\text{H}_2$ being the designed “reference”) was found to be enhanced by TiO_2 doping of the specimens to simulate ^6Li -burn-up expected to reach 20% at their end-of-life. The reaction rates, however, were so slow to be not significantly extrapolated to the breeder material service time (years). In $\text{Ar}+3\%\text{H}_2$, faster reaction rates allowed a better identification of the process evolution (kinetics) by “Temperature-Programmed Reduction”(TPR) and “Oxidation”(TPO), and combined TG-DTA thermal analysis.

The reduction of pure $\text{Li}_{4/5}\text{TiO}_{12/5}$ spinel phase to $\text{Li}_{4/5}\text{TiO}_{12/5-y}$ was found to reach in one day the steady state at the O-vacancy concentration $y=0.2$. Complimentary microscopy (SEM) and spectroscopy (XRD, XPS) techniques were used to characterize the reaction products among which the presence of the orthorhombic Li_vTiO_2 ($0 \leq v \leq 1/2$) and Li_2TiO_3 could be diagnosed. So that the complete spinel reduction to $\text{Li}_{1/2}\text{TiO}_2$ was obtained according to a scheme involving the $\text{Li}_{1/2}\text{TiO}_2$ - $\text{Li}_{4/5}\text{TiO}_{12/5}$ spinel phase solid solution for which $y=3v/(10-5v)$. The reduction rate of pure meta-titanate to $\text{Li}_2\text{TiO}_{3-x}$ was found much lower ($x \approx 0.01$) and even possibly due to the presence of the spinel phase whose quantitative determination (α_0 mol fraction) could not made below few%.

The TiO_2 doped Li-titanate ceramics were found to be reduced to an “average” Ti oxidation number $V_i=3.5+1/4(\text{Li}/\text{Ti})$ in the wide range (from 0 to 2) of Li/Ti atom ratio as corrected of Li-loss (corresponding to $\alpha=\alpha_0+\Delta\alpha$ increase) during testing. This Li-deficiency in Li_2TiO_3 ($0.8 \leq \text{Li}/\text{Ti} < 2$) was found to act as a “rate determining factor” of their reduction by a mechanism attributing to near the sole amount of spinel phase they contain (α) as fully reduced to $\text{Li}_{1/2}\text{TiO}_2$ as observed for the pure spinel phase alone.

Keywords: Fusion Power Plants, Breeding Blanket, Lithium Titanate (Li_2TiO_3), Pebble, Reduction, Oxidation

This is a report of the Working Group between ENEA (EU) and JAERI (JA) under the IEA Co-operative Programme on Nuclear Technology of Fusion Reactors.

* :Ente per le Nuove tecnologie, l'Energia e l'Ambiente (ENEA)
(C.R. Casaccia - Via Anguillarese, 301 00060 Roma, Italy)

核融合炉実証炉の増殖ブランケットに関連する熱化学環境下での 水素とチタン酸リチウムの反応に対するリチウムの減損効果

日本原子力研究所那珂研究所核融合工学部

Carlo ALVANI*・Sergio CASADIO*・Vittoria CONTINI*・Rossella GIORGI*

Maria Rita MANCINI*・土谷 邦彦・河村 弘

(2005 年 5 月 16 日受理)

本報告書は、国際エネルギー機関（IEA）の「核融合炉工学に関する協力研究協定」に基づいて実施した固体増殖ブランケット開発に関するサブタスクのワーキンググループの報告書である。このワーキンググループ（タスク F 及び WG-F）は、欧州と日本の間で 2000 年から 2004 年に行われ、熱化学環境下での水素とチタン酸リチウム（ Li_2TiO_3 ）との反応に関するリチウム減損効果について議論したものである。

Li_2TiO_3 と水素との反応は、核融合炉で設計されている増殖ブランケットの最も高温の微小球充填体領域に関して熱化学環境を模擬した条件で行った。900°C で $\text{Ar}+0.1\%\text{H}_2$ スイープガス（標準組成： $\text{He}+0.1\%\text{H}_2$ ）中の還元は、 Li_2TiO_3 の寿命である 20%-Li 燃焼度を模擬するために試料に TiO_2 を添加することにより行った。しかしながら、この反応速度は遅く、増殖材の使用期間（数年間）に対して意味ある外挿をすることができなかった。このため、 $\text{Ar}+3\%\text{H}_2$ スイープガス中で加速試験として昇温還元（TPR）・酸化（TPO）を行い、TG-DTA 熱分析により反応過程の確認を行った。

スピネル型 $\text{Li}_{4/5}\text{TiO}_{12/5}$ の $\text{Li}_{4/5}\text{TiO}_{12/5-y}$ への還元は、1 日間で $y=0.2$ の定常状態に到達することが分かった。補足的な観察（SEM）や分光分析（XRD 及び XPS）技術が、 Li_vTiO_2 （ $0 \leq v \leq 1/2$ ）や Li_2TiO_3 の存在を確認するために使用された。スピネル型 $\text{Li}_{4/5}\text{TiO}_{12/5}$ の完全な $\text{Li}_{1/2}\text{TiO}_2$ への反応は、 $y=3v/(10-5v)$ の関係をもつ $\text{Li}_{1/2}\text{TiO}_2$ - $\text{Li}_{4/5}\text{TiO}_{12/5}$ 固溶体を含んだ体系により得られた。一方、 Li_2TiO_3 から $\text{Li}_2\text{TiO}_{3-x}$ への還元反応は非常に小さい（ $x \approx 0.01$ ）ことが分かった。

TiO_2 添加 Li_2TiO_3 は、試験中、Li 損失（スピネル相成分： $\alpha = \alpha_0 + \Delta\alpha$ の増大に関連）による Li/Ti 原子比の広い範囲（0~2）において、平均 Ti 酸化数 $V_i = 3.5 + 1/4(\text{Li}/\text{Ti})$ の関係で還元されることが分かった。この Li_2TiO_3 中の Li 欠損（ $0.8 \leq \text{Li}/\text{Ti} < 2$ ）は、スピネル型 $\text{Li}_{4/5}\text{TiO}_{12/5}$ から $\text{Li}_{1/2}\text{TiO}_2$ への反応による還元メカニズムの「律速要因」であることが分かった。

核融合炉工学に関する IEA 国際協力研究協定に基づいて、ENEA（欧州）と原研（日本）間で実施したワーキンググループの報告書である。

那珂研究所（大洗駐在）：〒311-1394 茨城県東茨城郡大洗町成田町新堀 3607

* 新技術・エネルギー環境公社（イタリア）

Contents

Riassunto	1
1. Introduction	2
2. Experimental	3
2.1 Materials	3
2.2 Apparatus and Test of Temperature-Programmed Desorption (TPD), Reduction (TPR) and Oxidation (TPO)	3
2.3 Thermogravimetric and Differential Thermal Analysis (TG-DTA)	4
2.4 X-ray Diffraction (XRD) Analysis	4
2.5 X-ray Photoelectron Spectroscopy (XPS)	4
3. Results and Discussion	4
3.1 Reduction of Pure Materials	4
3.1.1 Titanium Oxide (TiO_2)	4
3.1.2 Meta-Lithium Titanate (Li_2TiO_3)	4
3.1.3 Spinel Phase Lithium Titanate ($\text{Li}_4\text{Ti}_5\text{O}_{12}$)	5
3.2 Reduction of TiO_2 Doped Li-Ti Pebbles and Pellets	8
4. Conclusion	9
References	11
Appendix I : Kinetic Elaboration by Thermogravimetric Tests	23
Appendix II : Results in This Collaboration	28

目 次

要約（イタリア語）	1
1. 序 論	2
2. 実 験	3
2.1 試 料	3
2.2 昇温脱着（TPD）・還元（TPR）・酸化（TPO）の試験装置と試験	3
2.3 示差熱分析（TG-DTA）	4
2.4 X線回折（XRD）	4
2.5 X線光電子分光分析（XPS）	4
3. 結果及び考察	4
3.1 純材料の還元	4
3.1.1 酸化チタン（ TiO_2 ）	4
3.1.2 メタ-チタン酸リチウム（ Li_2TiO_3 ）	4
3.1.3 スピネル型チタン酸リチウム（ $\text{Li}_4\text{Ti}_5\text{O}_{12}$ ）	5
3.2 TiO_2 添加 Li_2TiO_3 微小球及びペレットの還元	8
4. 結 論	9
参考文献	11
付録Ⅰ 示差熱試験による動的評価	23
付録Ⅱ 共同研究による成果	28

Acronyms and Definitions

EU :	European Union
JA :	Japan
HCPB:	Helium Cooled Pebble Blanket
FPY :	Full power Year
S.A.:	Surface Area
G.S.:	Grain Size
T.D.:	Theoretical Density
FWHM :	Full Width at Half Maximum
TPD:	Temperature-Programmed Desorption
TPR:	Temperature-Programmed Reduction
TPO:	Temperature-Programmed Oxidation
TG:	Thermogravimetry
TG-DTA:	Thermogravimetric and Differential Thermal Analysis
XRD:	X-ray Diffraction
XPS:	X-ray Photoelectron Spectroscopy
SEM :	Scanning Electron Microscopy
FWO :	Flynn-Wall-Ozawa
KAS :	Kissinger-Akahira-Sunose
α :	Fraction of Spinel Phase $\text{Li}_4\text{Ti}_5\text{O}_{12}$ in Lithium Titanate
β :	Heating Rate ($^{\circ}\text{C}/\text{min}$)
Δ :	Average ionic Valence Decrement in "reduced" Titanate from the Ti^{+4} Oxidation State ($\Delta=0.5$ means $\text{Ti}^{+3.5}$)
q :	Degree of Conversion
$\theta(t)$:	Diagnostic Diffusion Control of the Reaction Rate (Time-dependent)
$\theta(T)$:	Degree of Conversion (Temperature-dependent)
$f(\theta)$:	Differential Conversion Function
$g(\theta)$:	Defined by the Equation (10)

This is a blank page.

Li Depletion Effects on Li_2TiO_3 Reaction with H_2 in Thermo-chemical Environment Relevant to Breeding Blanket for Fusion Power Plants

Carlo Alvani, Sergio Casadio, Vittoria Contini, Rossella Giorgi, Maria Rita Mancini,
Kunihiko Tsuchiya* and Hiroshi Kawamura*

ENEA, C.R. Casaccia, uts MAT; *) Naka Fusion Research Establishment (Oarai-site), JAERI

Riassunto

Questo lavoro è stato effettuato dal “Subtask Group on Solid Breeder Blankets” nell’ambito del “implementino Agreement on a Co-operative Programme on Nuclear Technology of Fusion Reactors (International Energy Agency)”. Questo gruppo di lavoro (Task F and WG-F) fu costituito dal 2000 al 2004 tra EU e JA. In questo rapporto furono discussi gli effetti della deplezione del litio sulla reazione del titanato di litio (Li_2TiO_3) con idrogeno (H_2) in ambiente termochimico.

La reazione di ceramici di Li_2TiO_3 con idrogeno è stata studiata in un ambiente termo-chimico simulante (eccetto l’irraggiamento) quello della zona più calda del “breeding-blanket” attualmente in progetto per i reattori a fusione di potenza. Questa “riduzione” effettuata a 900°C in gas di lavaggio $\text{He}+0.1\%\text{H}_2$ ($\text{He} + 0.1\%\text{H}_2$ essendo la specifica di progetto) fu trovata aumentare con il drogaggio in TiO_2 dei campioni preparati per simulare il “Li-burn-up” previsto raggiungere il 20% a fine-vita. Tuttavia le velocità di reazione erano così basse da non poter essere estrapolate in modo significativo ai tempi di servizio (anni) di questi materiali. In $\text{Ar}+3\%\text{H}_2$ velocità di reazioni più alte consentirono una migliore identificazione dell’evoluzione del processo mediante metodi TPR/TPO ed analisi termica TG-DTA combinate.

La riduzione di fase pura $\text{Li}_{4/5}\text{TiO}_{12/5}$ spinello a $\text{Li}_{4/5}\text{TiO}_{12/5-y}$ fu trovata raggiungere lo stato stazionario in un giorno per una concentrazione di vacanze-O pari a $y = 0.2$.

Tecniche microscopiche (SEM) e spettroscopiche (XRD, XPS) furono impiegate per la caratterizzazione dei prodotti di reazione tra i quali fu diagnosticata la presenza di bronzi ortorombici Li_vTiO_2 ($0 \leq v \leq 1/2$) e di Li_2TiO_3 . Così che si ottenne la riduzione completa dello spinello a $\text{Li}_{1/2}\text{TiO}_2$ in accordo allo schema che coinvolge la soluzione solida $\text{Li}_{1/2}\text{TiO}_2$ - $\text{Li}_{4/5}\text{TiO}_{12/5}$ in fase spinello per la quale $y = 3v/(10-5v)$.

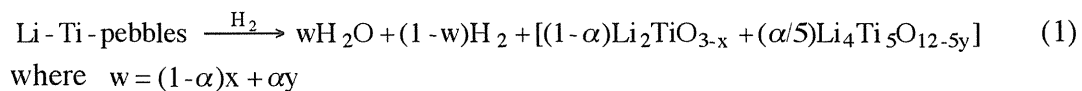
La riduzione di meta-titanate puro a $\text{Li}_2\text{TiO}_{3-x}$ fu trovata molto inferiore ($x \approx 0.01$) e perfino attribuibile alla presenza di fase spinello la cui determinazione quantitativa (α_0 frazione molare) non poté essere effettuata al di sotto di alcuni %.

I ceramici in Li-titanato drogati con TiO_2 furono trovati essere ridotti ad un valor medio del numero di ossidazione del Ti pari a $V_i = 3.5 + 1/4(\text{Li}/\text{Ti})$ per un ampio intervallo (da 0 a 2) dei rapporti atomico Li/Ti corretto delle perdite di Li (corrispondenti all’aumento $\alpha = \alpha_0 + \Delta\alpha$) durante le prove. Questa deficienza in Li in Li_2TiO_3 ($0.8 \leq \text{Li}/\text{Ti} < 2$) fu trovata funzionare da “fattore determinante la velocità” della loro riduzione mediante un meccanismo che attribuisce alla fase spinello in essi contenuto (α) la completa riduzione a $\text{Li}_{1/2}\text{TiO}_2$ come osservato per la sola fase spinello.

1. Introduction

This work was carried out under the Working Group in the Subtask on Solid Breeder Blankets in the Implementing Agreement on a Co-operative Programme on Nuclear Technology of Fusion Reactors (International Energy Agency (IEA)). This Working Group (Task F and WG-F) was performed from 2000 to 2004 by a collaboration of European Union (EU) and Japan (JA). In this report, lithium depletion effects on lithium titanate (Li_2TiO_3) reaction with hydrogen (H_2) in thermo-chemical environment were discussed.

Li_2TiO_3 ceramics (in form of dense pebbles) are candidate tritium breeding materials for the future fusion reactor power plants [1]. Tritium generation by the neutron capture reaction, ${}^6\text{Li}(n, \alpha)\text{T}$, deposits 4.8 MeV inside the Li_2TiO_3 (Li-Ti) pebble bed up to a Li-burn-up BU $\approx 20\%$ at high temperatures as 900°C [2]. Because of the high ${}^6\text{Li}$ cross section, the self-shielding makes it impossible to reach simultaneously both these extreme temperature-BU top values by irradiation tests performed in fission neutron reactors, unless high flux fast neutron sources are used [3]. The pebbles are swept by He purge with H_2 added to improve the tritium recovery rate [4]; and a “dry” He+0.1% H_2 as “reference” (R) purge gas has been selected as a compromise to recover tritium with an isotopic dilution as low as possible. This R-gas was found to interact with Li-Ti pebbles at temperatures from about 650°C . Its reducing effect could be measured at 800°C , and the involved Li-Ti pebbles restructuring showed consequences on their tritium release properties [5]. The rate of this process was found to depend on the pebble fabrication route, in particular on the Li/Ti atomic ratio that is generally kept below the stoichiometric value. For example, a 5% of TiO_2 doping is required for the “reference” HCPB-Li-Ti pebbles [6]. This TiO_2 -doping vs. reduction rate correlation was clearly stated by Tsuchiya et al. [7] that suggested how the presence of the $\text{Li}_4\text{Ti}_5\text{O}_{12}$ spinel phase inside the Li-depleted pebbles should be the key to find a realistic reaction scheme like (1) to study this phenomenon. Therefore, we considered the Li-Ti-pebbles as “composite” ceramic material having a fraction α of spinel phase (per Ti atom formula) in equilibrium with the monoclinic lithium meta-titanate phase



The variables x and y of eq. (1) are functions of the exposure time (t), temperature (T) and H_2 partial pressure, while α depends on the fabrication route (initial value α_0) and on Li-loss during service life.

The aim of the present work is to study the Li-Ti pebbles interaction by the scheme (1). Temperatures of $900\text{--}1000^\circ\text{C}$ for Knudsen effusion tests are too low to evaluate the Li-ceramic stability. On the contrary, they are too high for classical temperature programmed reduction (TPR) methods allowing high sensibility and precision in the gas phase composition analysis during the reaction to get the experimental variable $w(t)$. The solid phase changing can be followed by thermogravimetric and differential thermal analyses (TG-DTA) method covering correctly the needed temperature range to be explored but with a lower sensibility. In this work, the classical TPR was forced to work at 900°C in examining Li-depleted Li-Ti ceramics while pure phase powders were tested by TG-DTA at $1,000^\circ\text{C}$.

The envisaged service life of a power plant blanket is 3-4 years (FPY), a time scale not accessible by normal laboratory experiments. So we increased the H_2 concentration in the inert purge gas to improve the rate of eq.(1) by keeping the temperatures of technical interest and by neglecting the consequent variations or the reaction products of eq.(1). This is a hard hypothesis, since eq.(1) is determined by the reduction power of the environment which depends not only on the H_2 concentration in the inert gas but also on its gaseous impurities (H_2O , O_2 , CO , CO_2 , etc.)

and even the nature of the reaction vessel (quartz, steel, platinum, etc.). The reduction power in our tests was checked by reducing pure TiO_2 to TiO_{2-x} as a well supported thermodynamic data system [8].

2. Experimental

2.1 Materials

Two different Li_2TiO_3 pebble batches were prepared as reported in ref. [9] (citrate route) and were sintered at A) $1100^\circ\text{C} \times 2 \text{ h}$ (code FN6A-1100) and at B) $1300^\circ\text{C} \times 2 \text{ h}$ (FN6A-1300), respectively. This last treatment involved a reversible monoclinic-to-cubic transition of Li_2TiO_3 and induced a significant grain growth and lithium loss. A fine $\text{Li}_4\text{Ti}_5\text{O}_{12}$ powder [10] was also examined. A spinel-metatitanate biphasic composite (55% and 45% mol fractions, respectively, called “mixture” in the following (Table 1)) was prepared by reacting Li_2CO_3 with TiO_2 . The microstructures of the pebble-specimen surfaces were analyzed by scanning electron microscopy (SEM, Cambridge stereo-scan 250-MK3).

The powder-specimens were characterized for specific surface area (S.A.) by a NOVA-2200e analyzer (static method) and by the Quantachrome (Quantasorb-Quantector) system (dynamic method).

The tests were performed for a series of TiO_2 doped Li-Ti ceramics, including pure spinel phase. Un-doped Li_2TiO_3 and TiO_2 -doped Li_2TiO_3 pellets with various TiO_2 contents (8 mm diameter by 2 mm thickness) were fabricated with nearly the same density (about 83 % of T.D.) and microstructure (grain size (G.S.) from 1 to 2 μm). Un-doped Li_2TiO_3 and TiO_2 doped Li_2TiO_3 pebbles with various TiO_2 contents (about 1 mm in diameter) were also fabricated by the wet process. The details concerning their fabrication, characterization and XRD-patterns of these specimens listed in Table 1 have been reported in refs. [7, 11]. Photographs of the specimens in this study are shown in Figure 1. The microstructures of the pebble and pellet specimens analyzed by SEM are shown in Figure 2.

A specimen of highly Li-depleted Li-Ti pebbles was obtained as a by-product of the reference HCPB Li-Ti pebbles reprocessing [8], consisting of the original pebbles which have lost 85% of Li content in the nitric acid (HNO_3) dissolution bath (Li-depleted CTI, Table 1).

2.2 Apparatus and Test of Temperature-Programmed Desorption (TPD), Reduction (TPR) and Oxidation (TPO)

The TPD-TPR-TPO equipment and methods to study the Li-ceramic pebbles reaction (reduction) with the R-gas have been reported elsewhere [4,7]. In this work TPR runs were performed by imposing an isothermal-annealing run at 900°C to the specimens exposed to flowing (40 cm^3/min) hydrogen doped purge gas after their preliminary “cleaning” by a TPD consisting in ramp-annealing runs to remove H_2O and CO_2 impurities from their surfaces [7].

The amount of H_2 consumed = H_2O generated are expressed in mole per Ti-atom in order to have a direct measure of the reduction degree of titanium, which was assumed not to leave the solid lattice during the process (while oxygen and lithium can do). The Li vapor formation was considered to be irreversibly lost during the TPR runs (because of mass-transfer in the quartz reaction tubes). On the contrary, O-loss during TPR was reversibly recovered during the TPO runs imposed on the reduced products of the preceding TPR runs without removing the specimen from the measuring cell. They consisted in annealing ramp (heating rate $\beta=10^\circ\text{C}/\text{min}$) by sweeping $\text{He}+0.1\% \text{ O}_2$ or $\text{Ar}+1.5\% \text{ H}_2\text{O}$ oxidizing gas mixtures. The calibration of this procedure was tested (Figure 3 [12]) on a pure Ti_2O_3 containing the fully reduced Ti^{3+} ions. The mechanism appears different for the two oxidizing mixtures. However, the areas of the two TPO spectra correspond to the same charge needed to $\text{Ti(III)} \rightarrow \text{Ti(IV)}$ full conversion, and the

quantitative determination of Ti^{3+} in titanium oxides was set-up. In practice the use of H_2O -doped Ar mixture was more convenient than that of O_2 -doped He in performing the experimental sequence TPR \rightarrow TPO. Unbalance between TPR and the TPO charges (always $\text{TPR} \geq \text{TPO}$) was attributed to Li-loss.

2.3 Thermogravimetric and Differential Thermal Analysis (TG-DTA)

TG and DTA were carried out simultaneously by a Netzsch STA 409 instrument with its high temperature furnace. The equipment was previously evacuated and filled with Ar up to oxygen elimination in the reaction chamber. Powdered samples (140-160 mg) were heated and cooled in Pt crucibles at rates β varying from 2 to $10^\circ\text{C}/\text{min}$ from room temperature up to 1350°C .

2.4 X-ray Diffraction (XRD) Analysis

XRD spectra were obtained using Cu-K α radiation in a Bragg-Brentano powder diffraction-meter equipped with a graphite monochromator positioned in the diffracted beam. No evidence for any secondary phases was found in $\text{Li}_4\text{Ti}_5\text{O}_{12}$ powder, indicating that this was a pure spinel phase sample. The cell parameter, calculated using the Unitcell program, was 8.347 Å, in good agreement with the theoretical value ($a=8.357$ Å JCPDS card 72-0426).

2.5 X-ray Photoelectron Spectroscopy (XPS)

XPS measurements were performed with a V.G. ESCALAB Spectrometer. Detailed spectra were acquired at 20 eV pass energy, which gave rise to a $\text{Ag}3d_{5/2}$ peak with 1.2 eV in full width at half maximum (FWHM). Powdered samples were pressed in a proper stainless steel sample holder in order to minimize charging effects due to weak contact with the spectrometer.

3. Results and Discussion

3.1 Reduction of Pure Materials

3.1.1 Titanium oxide (TiO_2)

Reduction of pure TiO_2 anatase fine powder to TiO_{2-x} was tested to check the reduction power of our experimental reaction chambers in which $\text{Ar}+3\%\text{H}_2$ was flowing during the reduction-annealing tests.

The TPR runs were performed in quartz U-tubes in which the TiO_2 anatase oxide (Table 1) was reduced to $\text{TiO}_{1.75}$ or to Ti_4O_7 Magneli phase ($x = 1/n = 0.25$). The p-T diagrams for $\text{Ti}_4\text{O}_7/\text{Ti}_5\text{O}_9$ equilibrium [8] at 900°C show that the oxygen partial pressure p should range within $10^{-18} \leq p < 10^{-17}$ Pa ($10^{-23} \leq p < 10^{-22}$ atm) in our TPR runs.

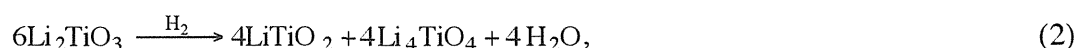
The TG-DTA tests were performed on powder specimens put on platinum crucibles exposed in free static air. Their reduction was examined in flowing ($100 \text{ cm}^3/\text{min}$) $\text{Ar}+3\%\text{H}_2$ gas whose the reduction power gave $x = 0.18$, hence p to lie within $10^{-15} \leq p < 10^{-14}$ Pa ($10^{-20} < p < \sim 10^{-19}$ atm) at 1000°C .

3.1.2 Meta-Lithium titanate (Li_2TiO_3)

The scheme (1) with no spinel presence ($\alpha = 0$) leads to $w = x$. It is convenient to use a parameter $\Delta = 2x$ directly connected to the Ti valence decrease from the fully oxidized value +4 during reduction. Figure 4 shows the evolution of Δ for “nominal” stoichiometric Li_2TiO_3 FN6A-1100 (Table 1) and JPBL-0 (mentioned in Tables 1 and 2) pebbles reduction to $\text{Li}_2\text{TiO}_{3-x}$ ($x=\Delta/2$) at 900°C in flowing $\text{Ar}+3\%\text{H}_2$ and in $\text{Ar}+0.1\%\text{H}_2$, respectively. The isochronal Δ values were found to increase nearly in direct proportion to H_2 partial pressure, unless Li-loss was observed to occur in the 3% H_2 -doped purge (last and higher part of the data). XRD, however,

cannot show the presence of spinel phase into the m-titanate at levels below few %, not to speak below 0.1% that should be responsible of the reduction observed. For example, TPR test of the FN6A-1300 pebbles in the R-purge (Ar+0.1%H₂) is also reported in Figure 4 to show how a few Li-loss due to heat treatments deeply affects (increases) the reduction rate. FN6A-1300 differs from FN6A-1100 only on the sintering treatment (1300°C×2 h) which involved the reversible monoclinic-to-cubic phase transition (m-Li₂TiO₃ → c-Li₂TiO₃) occurring above 1150°C [13], which improved grain growth (Figure 2) and Li-loss. But no spinel phase was detectable by XRD. The role played by the specimen microstructure seems to be not important: since the slightly Li-depleted FN6A-1300 undergoes a higher reduction rate, although its grains are larger than those of FN6A-1100 (Figure 4), which should have suggested a higher reaction rate for this last, while the contrary is observed. A nucleation of a fine dispersed phase at the grain surfaces of FN6A-1300 was also observed (Figure 4), but its level was too low to be detectable by XRD.

Kleycamp [13] claimed the following scheme (2) to hold as the most probable bulk-reduction mechanism for the pure Li₂TiO₃



in which the reduced LiTiO₂ product (containing Ti³⁺ ion, Δ=1) is accompanied by the formation of lithium orthotitanate (o-Li₄TiO₄) that could occur at temperatures for which Li₂TiO₃ may disproportionate in a solid solution extended from o-Li₄TiO₄ to R-Li₂Ti₃O₇ (ramsdellite type) phase. In the present TPR tests (900°C), we were far from this situation.

3.1.3 Spinel phase lithium titanate (Li₄Ti₅O₁₂)

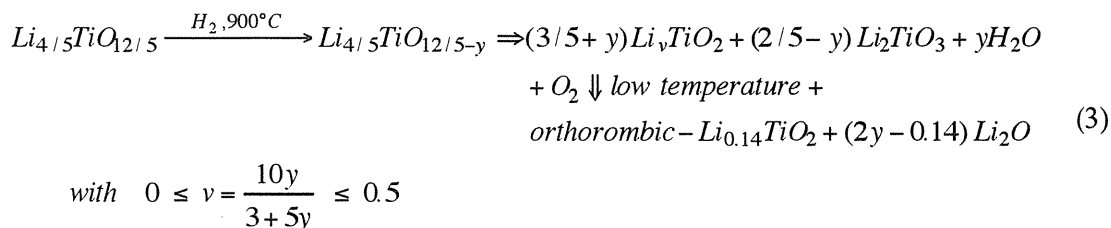
The scheme (1) for pure spinel phase (α=1) leads to w = y = Δ/2.

In the TPR-TPO tests, the reaction rates of pure spinel “pellets” when performed by Ar+3%H₂ gas sweeping at 900°C (Figure 5) were found remarkably higher than that observed for fine “powder” (IT-SP) as swept by Ar + 0.1% H₂. No Li-loss was observed during the runs, indicating the value Δ ≈ 0.3 (y = 0.15) as best fitting the curve at equilibrium.

It is known that the spinel oxides Li_{0.5}TiO₂ and Li_{4/3}Ti_{5/4}O₄ (≡ Li₄Ti₅O₁₂) are the end members of the solid solution series Li_{1+z}Ti_{2-z}O₄ with 0 ≤ z ≤ 1/3 [10,14-18] involving a decrease in Li/Ti ratio while the reduction increases.

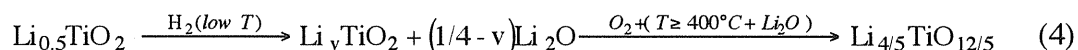
Very interesting was the XRD analysis (Figure 5-B) of the reaction products showing the presence of m-Li₂TiO₃ among them due to the peak for 2θ = 20.5° which exists only for this compound in the Li-Ti-O ternary system data-files. All the other peaks of this phase were also recognized to be present; and the resulting cell parameters (a=5.097Å, b=8.78Å, c=9.75Å, β=100.5°) as compared to the standard ones (a_T=5.069Å, b_T=8.799Å, c_T=9.759Å, β=100.2°) give a cell volume slightly larger than the theoretical value. This is because its formulation as Li₂TiO_{3-x} is suggested to hold for very low x (Ti⁴⁺ in this phase remains nearly unchanged inside this “reduced” product).

The relations (3) follows the scheme (1) for α=1 (pure spinel) by assuming co-produced m-Li₂TiO₃ as not reducible by (2); this means that we got the Li_{0.4}TiO₂ product (cubic-spinel, 75% mol fraction with an average Ti oxidation number (No.) =+3.6) accompanied by m-Li₂TiO₃ (25% mol fraction) as confirmed by XRD analysis)



The XRD pattern of Figure 5-B showed the presence of orthorhombic $\text{Li}_{0.14}\text{TiO}_2$, a phase known to be generated from Li_vTiO_2 “bronzes” ($0.14 \leq v \leq 0.5$) exposed to free air at room temperature [14,15]. This degradation involves further Li-oxide phase generation (as sketched by the vertical arrow in the scheme (3)) that occurred on sight during XRD measurements. The consequent Li_2O transport at the air-aged grain surfaces was well detected by XPS (Figure 5-C) showing a very high Li-surface concentration on the reaction products.

The TPO run in Figure 6 [12] refers to a similarly TPR reduced specimen not removed from its reaction vessel. It shows several peaks corresponding to a step-wise re-oxidation up to fully reversion of (3) for $T \geq 400^\circ\text{C}$ in 0.1% O_2 (scheme (4)) or for $T \geq 700^\circ\text{C}$ in 1.5% H_2O -doped Ar gas.



The kinetics of the process (3) was evaluated by elaborating the data plotted in Figure 5-A by assuming diffusion rate control for the fractional reaction advancement $\theta(t)$. The $\theta(t)$ is given by the classical solution (5) of the boundary diffusion problem for spherical geometry by assuming a as diffusion path (spherical radius) and D as effective diffusion coefficient both unknown but connected to the observable rate constant k by the relationship (6),

$$\theta(t) = \frac{\Delta(t)}{\Delta_{(\text{equilibrium})}} = \left[1 - 6/\pi^2 \sum_{n=1}^{\infty} n^{-2} \exp(-n^2 t / \tau) \right] \quad (5)$$

$$\tau = \frac{\pi^2 a^2}{D} \approx \frac{1}{k} \quad (6)$$

For $t \leq \tau$ the good approximation of (5):

$$\theta(t) = 4\sqrt{\frac{t}{\tau}} - \frac{3t}{2\tau}$$

puts in evidence the initial square root $\theta(t)$ time dependence to diagnostic diffusion control of the reaction rate. That was indeed observed in the plots reported in Figures 4-A and 5-A (slope 1/2 of log-log plots).

The eq.(5) gave the best fitting to the data for $\tau=15\text{h}$ and $\tau=300\text{h}$ (Figure 5) for $\text{Ar}+3\%\text{H}_2$, and in $\text{Ar}+0.1\%\text{H}_2$, respectively; and the k increase of a factor 20 was quasi proportional to that of H_2 concentration (a factor 30).

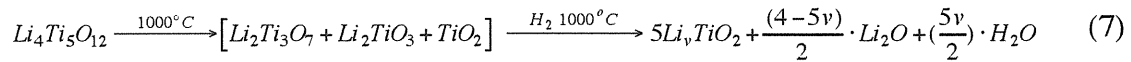
The study of spinel phase reduction at 1000°C was not accessible to our TPR device. It could be approached by TG technique with the advantage to explore endo- and exo-thermal transitions by simultaneous DTA.

Figure 7 shows the weight loss of the spinel powder due to its reduction in flowing $\text{Ar} + 3\%\text{H}_2$ ($100 \text{ cm}^3/\text{min}$) during the heating ramp ($\beta=10^\circ\text{C}/\text{min}$) starting from room temperature up to 1200°C . The DTA signal puts in evidence the presence of an endo-thermal peak (1021°C)

overlapping that of the spinel ($\text{Li}_4\text{Ti}_5\text{O}_{12}$) decomposition to ramsdellite $\text{R-Li}_2\text{Ti}_3\text{O}_7 + \text{c-Li}_2\text{TiO}_3$ solid solution [13] involving a simultaneous weight loss rate increase (note the slope variation of the TG signal at $\sim 1020^\circ\text{C}$). During the successive cooling ramp ($\beta = -10^\circ\text{C}/\text{min}$), the observed exo-thermal peak (907°C) could be assigned to the reverse transition changed by the reduction-annealing performed up to 1200°C . This peak was indeed observed also during cooling in the same way reduced-annealed specimens held at 1000°C for 17 h in such environment (isothermal reduction-annealing runs, Figure 8), which is a strong indication that this transition was occurring as overlapped to the reduction process.

The mixture powder was also tested by TG-DTA (Figure 7), and a more complex DTA signal was observed with two endo-thermal phase transitions (at 971 and 1066°C) suggesting that the spinel decomposition step is accompanied by the reversible monoclinic-cubic $\text{m-Li}_2\text{TiO}_3 \rightarrow \text{c-Li}_2\text{TiO}_3$ phase transition which should start at 930°C and completed above 1008°C following the Izquiero-West and Mikkelsen phase diagram used by Kleykamp [11]. A steep increase in the weight loss rate was observed to start at $\sim 1050^\circ\text{C}$, corresponding to this phase transition for both spinel and mixture specimens.

The Figure 8 [19] reports the weight losses of the spinel and mixture specimens (as corrected for Li-loss) observed during the reduction annealing in $\text{Ar}+3\%\text{H}_2$ held 17 h at 1000°C (lower curve). The final weight loss for spinel was 1.1% and its extrapolation to equilibrium gave 1.24% following the scheme (7) by which resulted an average $V_i = 3.86$ ($\Delta = v = 0.14$).



In this case, in fact no Li_2TiO_3 phase could be detected by XRD analysis of the products, indicating that not only the Ramsdellite was involved in the reduction leading to a complete decomposition of the original spinel phase into the orthorhombic $\text{Li}_{0.14}\text{TiO}_2$ and Li_2O as shown by XRD and XPS analysis of Figure 9 [19]. The weight loss of mixture powder (as performed in the same conditions, also reported in Figure 8) was observed to evolve similarly by an extent proportional to the concentration of spinel phase. This difference corresponds to the spinel phase fraction (60%). That suggests how meta-titanate phase in this composite specimen is not significantly reduced even at 1000°C annealing step (according also to XRD analysis of the reaction products).

The reduction kinetics of such a very complex process was evaluated by classical TG isothermal and non-isothermal methods reported in Appendix. The $\theta(t)$ function is now referred to the fractional weight change (8)

$$\theta(t) = \frac{W(t) - W_o}{W_\infty - W_o}, \quad (8)$$

where W_o , $W(t)$ and W_∞ are the initial, actual and final mass, respectively, during the reduction of spinel following the scheme (7). The rate of reaction (9)

$$\frac{d\theta(t)}{dt} = Kf(\theta(t)) = A \exp\left(-\frac{E}{RT}\right) f(\theta(t)) \quad (9)$$

is a formula in which the reaction rate constant K is assumed to follow an Arrhenius type thermally activated law (A = frequency factor, E = activation energy, R = gas constant, T = Kelvin degrees temperature); $f(\theta)$ is a differential conversion function depending on reaction mechanism (see Appendix) where $g(\theta)$ integrals (10) are formulated for the different reaction types (Table A1).

$$g(\theta) = \int_0^\alpha \frac{d\theta}{f(\theta)} = K \int_0^t dt \quad (10)$$

Excepting the small range 0.34-0.40 corresponding to a flattening of θ (Figure 10 [19]), the reaction rates are of the same order of magnitude and are similar for both the specimens. They seem to be initially reduced by different mechanisms; the pure spinel follows diffusive type steps (according to TPR tests at 900°C), while in the other cases (R2-R3) the geometric growth of the reaction interface is the rate controlling process.

In any case, it could be stated that the reduction of the mixture specimen has to be attributed mainly to its spinel phase component.

In non-isothermal conditions the kinetic analysis is performed by the equation (11) obtained from (10) with θ formulated as function of temperature ($T=T_0+t$).

$$\beta \frac{d\theta}{dT} = Af(\theta) \exp\left(-\frac{E}{RT}\right) \quad (11)$$

The dependence of E on θ (Figure 11 [19]) was evaluated by iso-conversional integral methods (see Appendix I) by experimental $\theta(T)$ obtained at various β (Figure 12 [19]). The initial difference between the two specimens (for $0 < \theta < 0.4$) tended to decrease by increasing θ up to disappear (within the error of measurements) for $\theta \geq 0.8$ where $E \approx 250$ kJ/mol.

3.2 Reduction of TiO₂ doped Li-Ti pebbles and pellets

Figure 13 [20] shows the reduction evolution of few specimens selected as “typical” among all the investigated Li-Ti-ceramics (Table 1) by isothermal annealing TPR runs at 900°C in Ar + 3% H₂ flowing gases. This figure gives the results reported in Table 2 at the end of the tests (after 15-17 h or as extrapolated to the expected equilibrium).

The Li/Ti ratio of pebbles was spanning from 0.145 (Li-d-CTI) to 2 (JPBL-0). The reduction evolution for the last value (Li/Ti = 2) (Figure 13) corresponded exactly to that of observed for the pellets (PLT-0) already shown in Figure 4. These results demonstrated the reproducibility of the TPR measurements and the care applied in the fabrication of so different ceramic specimens (Table 2) by keeping the same microstructure.

The JPBL-10 specimens have a phase composition close to that expected at the end-of-life Li-burn-up of Li-Ti pebbles. For them it was possible to try the same kind of analysis performed for the pure spinel phase by the equations (5) and (6) in spite of a lower TPR signal and Li-loss detected only at the end of runs; the time constants for Ar+3% H₂ and Ar+0.1% H₂ were found to be $\tau = 5$ h and $\tau = 185$ h, respectively. Although the order of magnitude of these parameters agrees with that of the pure spinel pebbles, the slight higher rate constants involved some (significant) meta-titanate phase reduction to Li₂TiO_{3-x} (see the last column of Table 2). Li-loss was found randomly related to Li/Ti in the range $0.8 < \text{Li/Ti} \leq 2$ for which the two phase system of the m-Li₂TiO₃/Li₄Ti₅O₁₂-spinel keeps Li activity constant. For $\text{Li/Ti} \leq 0.8$ no Li-loss was observed by TPR tests, which suggested that the couple Li₄Ti₅O₁₂/TiO₂ fixed a much lower Li-activity of the system.

Following the scheme (1), the average Ti oxidation number V_i is related to those of Ti in the spinel (V_1) and in m-Li₂TiO₃ (V_2) phases by the implicit equation (12).

$$V_i = (1 - \alpha)V_2 + \alpha V_1 \quad (12)$$

For $\alpha=0$, we got $\alpha=0.01$ (Figure 4) hence $V_2=3.99$. To the other extreme of pure spinel phase $\alpha=1$, we got $\alpha=0.3$ (Figure 5) and $V_1=3.7$. Let us use these values to evaluate intermediate situations of composite specimen by the expressions

$$V_1 = [V_i - (1 - \alpha) \times 3.99] / \alpha = (V_i - 3.99) / \alpha + 3.99 \quad \text{and} \\ V_2 = [V_i - \alpha \times 3.7] / (1 - \alpha)$$

far from the limits $\alpha \rightarrow 0$ and $\alpha \rightarrow 1$ for which the right members diverge respectively.

The last two columns of Table 2 and Figure 14 report the so calculated average V_1 and V_2 values for spinel and Li-metatitanate reduced products.

These results show that the spinel phase is mainly responsible of the “bulk” reduction phenomenon of the Li-Ti pebbles. One of the reason of that could be attributed to the highly defective structure of the spinel phase in which Li^+ ions substitute 1/3 of the Ti^{4+} ions in their octahedral sites leaving void in half of all the Li^+ tetrahedral sites [14,15,21], and the redistribution of lithium ions upon heating makes this titanate much more reactive than the stable metatitanates or perovskites.

The plot of Figure 14 shows that as the equilibrium the “average” titanium oxidation numbers V_i of Li-titanates exposed to $\text{Ar}+3\%\text{H}_2$ is a linear function of the Li/Ti atom ratio (13).

$$V_i = 3.5 + \frac{1}{4}(\text{Li/Ti}) \quad \text{for } 0 \leq \text{Li/Ti} < 2.0 \quad (13)$$

Hoshino et al. obtained this kind of data by TG methods in flowing $\text{Ar}+20\%\text{H}_2$ at 800 and 1000°C [21, 22], which are also plotted in Figure 14; they nearly follow the trend of (13) in spite of the different environmental conditions which corresponded to an oxygen partial pressure $p = 10^{-19}$ Pa (10^{-24} atm).

4. Conclusion

Our scheme (1) which splits the Li-Ti-ceramics reduction into the two phases in thermodynamic equilibrium (“formally” $\text{Li}_2\text{TiO}_{3-x}$ and $\text{Li}_4\text{Ti}_5\text{O}_{12-5y}$) was tested at 900°C by reaching near steady state reaction in the reduction environment given by $\text{Ar}+3\%\text{H}_2$ purge gas. The oxygen vacancy concentration resulted to be $x = 0.005$ and $y = 0.15$, whatever the Li/Ti ratio (or spinel mol fraction α per Ti atom) is (Figure 14). At this temperature this formalism (typically used in solid-state-defect chemistry) was found effective only for the meta-titanate which resulted poorly reduced. On the contrary the spinel phase was found to decompose in a “bronze” Li_vTiO_2 ($0 \leq v \leq 1/2$) with Li_2TiO_3 (scheme (2)) with a sort of disproportion of Ti ions, Ti^{4+} in $m\text{-Li}_2\text{TiO}_3$ and $\text{Ti}^{3+}/\text{Ti}^{4+}$ 1:1 in $\text{Li}_{0.5}\text{TiO}_2$ that resulted to be the compound reduced at the maximum level in our TPR apparatus. This compound is a well known superconductor compound having Ti^{3+} and Ti^{4+} ions shared by “order” (1:1) on octahedral sites of the cubic Ti sub-lattice. This result was in agreement with results of reduction tests performed in the same environment on pure TiO_2 which led to T_4O_7 , also an ordered $\text{Ti}^{3+}\text{-Ti}^{4+}$ (1:1) Magneli phase.

Similar tests performed on fine spinel powders at 1000°C by TG-DTA showed a more complex reduction mechanism, although similar to that obtained for a spinel-metatitanate (near one-to-one mol) composite powder, which confirms the Li_2TiO_3 phase reduction as “negligible” even at this temperature. The time constant of these reactions was found to be of the order of a day which should increase to a month for a “reference” purge gas composition ($\text{He}+0.1\%\text{H}_2$) of the blanket technology.

The reduction rate of Li-Ti-ceramics at 900°C was influenced by their spinel phase $\text{Li}_4\text{Ti}_5\text{O}_{12}$ content depending in turn on the Li/Ti atom ratio. Even in Ar+0.1% H_2 (simulating “reference” purge gas) pure Li_2TiO_3 pebbles undergoing very low reduction rate (Figure 4) was suddenly attacked when modest Li-loss occurred. The Li/Ti atom ratio (due both to initial TiO_2 doping and to Li-loss during testing) was determined, the reduction rate how if a consequent spinel phase is soon generated at the grain boundary surface of the specimens. Since in Li-ceramic breeding blankets the Li-loss is mainly determined by ^6Li -burnup, the rate of this transmutation reaction will control the reduction attack that will be limited to the consequent spinel phase generated.

The reported kinetic parameters (characterizing this process) allow conservative extrapolations to 800°C for which negligible effects have to be envisaged for Li-Ti-pebbles exposed for a time comparable to the life in service (years) of this type of ceramic breeder materials. The radiation effects remain to be explored.

Note: Several of the present data have been reported (partially and in different forms) in recent international workshops on Ceramic Breeder Blanket Interactions (CBBI-11, Tokyo-2003 and CBBI-12, Karlsruhe-2004) whose proceedings are available as a Japan Atomic Energy Research Institute Report JAERI-Conf 04-012 (2004), pp.148-162.

References

- [1] P. Gierszewski, M. D. Donne, H. Kawamura, M. Tillack, *Fusion Eng. Des.* 27 (1995) 167.
- [2] L. V. Boccaccini, N. Bekris, Y. Chen, U. Fischer, S. Gordeev, S. Hermsmeyer, E. Hutter, K. Kleefeldt, S. Malang, K. Schleisiek, I. Schmuck, H. Schnauder, H. Tsige-Tamirat, *Fusion Eng. Des.* 61-62 (2002) 339.
- [3] G.W. Hollemberg, T. Kondo, H. Watanabe, R.J. Puigh, T.C. Reuther, *J. Nucl. Mater.* 155-157 (1988) 202-206.
- [4] S. Casadio, J.G. van der Laan, C. Alvani, A.J. Magielsen, M.P. Stijkel, *J. Nucl. Mater.* 329-333 (2004) 1252-1255
- [5] C. Alvani, P.L. Carconi, S. Casadio, N. Roux, *Fusion Eng. Des.* 58-59 (2001) 701.
- [6] J.D. Lulewicz, N. Roux, *J. Nucl. Mater.* 307-311 (2002) 803.
- [7] K. Tsuchiya, C. Alvani, H. Kawamura, H. Yamada, S. Casadio, V. Contini, *Fusion Eng. Des.* 69 (2003) 443.
- [8] P. Walzer and G. Eriksson, *Calphad* 23 (1999) 189. Or/and L.A. Bursil and B.G. Hyde, Crystallographic Shear in the Higher Titanium Oxides: Structure, Texture, Mechanisms and Thermodynamics, in "Progress in Solid State Chemistry", Vo. 7, H. Reiss and J.O.McCaldin editors, Pergamon Press.
- [9] C. Alvani, S. Casadio, V. Contini, A. Di Bartolomeo, J.D. Lulewicz, N. Roux, *J. Nucl. Mater.* 307-311 (2002) 837.
- [10] P.P. Prosini, R. Mancini, L. Petrucci, V. Contini, P. Villano, *Solid State Ionics*, 144 (2001) 185.
- [11] K. Tsuchiya, H. Kawamura, *Fusion Technology*, 39 (2001) 624.
- [12] C. Alvani, S. Casadio, V. Contini, R. Giorgi, M.R. Mancini, K. Tsuchiya, H. Kawamura, et al., "High temperature reactivity of Li-titanates with H₂ contained in purge gas," Proc. of the 11th International Workshop on Ceramic Breeder Blanket Interactions, JAERI-Conf 2004-012, (2004).
- [13] H. Kleykamp, *Fusion Eng. Des.* 61-62 (2002) 361. See also: H. Kleykamo, "Thermal properties of Li₂TiO₃ and phase equilibria in the Li-Ti-O system", in Proceedings of CBBI-10 (L. Boccaccini editor, FZK), Oct.22-24 (2001), Karlsruhe.
- [14] E. G. Moshopoulou, *J Am. Ceram. Soc.*, 82 (1999) 3317 (with 9 cited references on the argument).
- [15] J. Akimoto, Y. Gotoh, Y. Oosawa, N. Nanise, T. Kumagai, K. Aoki, H. Takei, *J. Solid State Chem.* 113 (1994) 27.
- [16] S. Satpathy, R.M. Martin, *Phys. Rev.* 36 (1987) 7269.
- [17] C.Chen, M. Spears, F. Wondre, J. Ryan, *Crystal Growth*, 250 (2003) 139.
- [18] K.M. Colbow, J.R. Dahn, R.R. Haering, *J. Power Sources*, 26 (1989) 397.
- [19] M.R. Mancini, V. Contini, K. Tsuchiya, et al., "Thermochemistry of Li-Titanates ceramics in reducing environments," The 23rd Symposium on Fusion Technology (SOFT-23), 2004, Venice, Italy, to be published in *Fusion Eng. Des.*
- [20] C. Alvani, K. Tsuchiya, V. Contini, F.Pierdominici, H. Kawamura, S. Casadio, "Kinetics of Li depleted Li₂TiO₃ reaction with H₂ added to Ar purge gas," The 23rd Symposium on Fusion Technology (SOFT-23), 2004, Venice, Italy, to be published in *Fusion Eng. Des.*
- [21] T. Hoshino, M. Dokiya, T. Terai, Y. Takahashi, M. Yamawaki, *Fusion Eng. Des.* 61-62 (2002) 353.
- [22] T. Hoshino, M. Yasumoto, Y Takahashi, T. Terai, M. Yamawaki, *J. Mass. Spectrom. Soc. Jpn* 51 (2003) 163.

Table 1 List and main characteristics of the examined titanium oxide specimens

Formula	Code	Density (%T.D.)	S.A. ¹ (m ² /g)	G.S. ² (μm)	Heat treat.	Phase composition by XRD
[Pebbles]						
					(sintering)	
Li ₂ TiO ₃	FN6A-1100	60.3	-	1-5	1100°C × 2h	m-Li ₂ TiO ₃
Li ₂ TiO ₃	FN6A-1300	69.0	-	5-20	1300°C × 2h	m-Li ₂ TiO ₃ + Li ₄ Ti ₅ O ₁₂ traces
Li ₂ TiO ₃	JPBL-0	82.3	-	2-7	1235°C × 15min	m-Li ₂ TiO ₃
(TiO ₂ : 0mol%)						
TiO ₂ - Li ₂ TiO ₃	JPBL-2.5	84.0	-	2-7	1170°C × 15min	m-Li ₂ TiO ₃
(TiO ₂ : 2.5mol%)						
TiO ₂ - Li ₂ TiO ₃	JPBL-5	81.7	-	2-7	1130°C × 15min	m-Li ₂ TiO ₃
(TiO ₂ : 5mol%)						
TiO ₂ - Li ₂ TiO ₃	JPBL-10	84.8	-	5-30	1210°C × 15min	m-Li ₂ TiO ₃ + Li ₄ Ti ₅ O ₁₂ traces
(TiO ₂ : 10mol%)						
Li-d-LiTi	Li-d-CTI	-	-	-		HCPB ref. LiTi pebbles Li-depleted in HNO ₃ solution, Li/Ti = 0.149
[Pellets]						
Li ₂ TiO ₃	JPLT-0	82-84	-	1.3	1076°C × 4h	m-Li ₂ TiO ₃
(TiO ₂ : 0wt%)				±0.4		
Li ₂ TiO ₃	JPLT-10	82-84	-	1.6	960°C × 4h	m-Li ₂ TiO ₃
(TiO ₂ : 10wt%)				±0.5		
Li ₂ TiO ₃	JPLT-20	82-84	-	1.6	960°C × 4h	m-Li ₂ TiO ₃ + Li ₄ Ti ₅ O ₁₂ traces
(TiO ₂ : 20wt%)				±0.4		
Li ₂ TiO ₃	JPLT-30	82-84	-	1.4	960°C × 4h	m-Li ₂ TiO ₃ + Li ₄ Ti ₅ O ₁₂ traces
(TiO ₂ : 30wt%)				±0.5		
Li ₄ Ti ₅ O ₁₂	JPLT-SP	82-84	-	0.9	960°C × 4h	Li ₄ Ti ₅ O ₁₂ spinel phase
				±0.5		
[Powders]						
					(reaction)	
Li ₄ Ti ₅ O ₁₂	Spinel [10]	-	7.56	0.2	800°C × 36h	pure Li ₄ Ti ₅ O ₁₂ spinel phase
Li ₄ Ti ₅ O ₁₂ + Li ₂ TiO ₃	Mixture	-	-	-	800°C × 36h	Composite Spinel (55%) - meta- titanate (45%)
TiO ₂	Aldrich-1317	-	14.7	0.1	-	anatase
Ti ₂ O ₃	Aldrich-1344	-	0.65	2	-	corundum type

1 : surface area, 2 : grain size

Table 2 Measured lithium loss and average Ti oxidation numbers V_i (both numbers are experimental data) in pebbles and pellets reduced in flowing Ar+3%H₂ at 900°C for 17 h and extrapolated at steady state.

Sample codes	Initial Li/Ti ($\pm 2\%$)	Li/Ti loss ($\pm 0.5\%$)	Li _{4/5} TiO _{12/5} fraction α ($\pm 2\%$)	Av. Ti oxidat. No. V _i ($\pm 0.5\%$) exp. 17 h st-state		Av. Ti oxidat. No. in the spinel phase (V ₁)	Av. Ti oxidat. No. in m-Li ₂ TiO ₃ phase (V ₂)
Pebbles							
JPBL-0	2.00	-0.017	0.014	3.99	3.99		3.99
JPBL-2.5	1.95	-0.024	0.062	3.98	3.98	3.83	4.00
JPBL-5	1.90	-0.005	0.11	3.95	3.95	3.63	3.98
JPBL-10	1.80	-0.019	0.18	3.93	3.93	3.66	3.98
Li-d-CTI				3.81	3.54		
TiO ₂ -an.	0	0	0	3.75	3.50		
Pellets							
JPLT-0	2.000	-0.017	0.014	3.99	3.99		3.99
JPLT-10	1.74	-0.005	0.225	3.91	3.91	3.69	3.97
JPLT-20	1.49	-0.020	0.44	3.87	3.86	3.69	3.99
JPLT-30	1.26	-0.011	0.63	3.84	3.81	3.70	4.00
JPLT-SP	0.80	0	1.00	3.74	3.70	3.70	

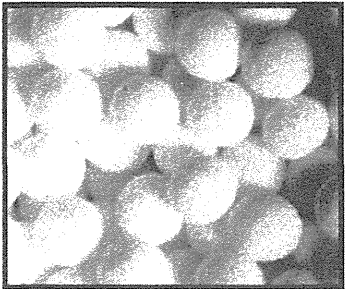
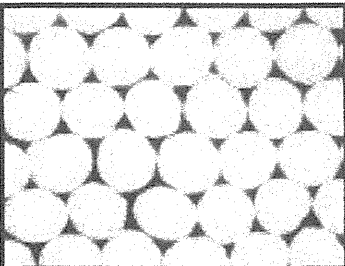
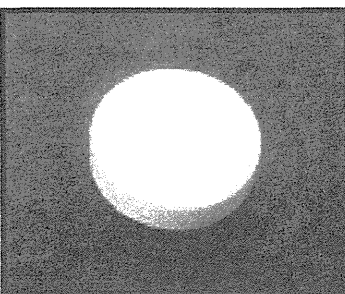
Code No.	Photograph	Shape (mm)	Remarks
FN Series		Pebble (~ $\phi 1$)	Li_2TiO_3 pebbles obtained by powder agglomeration in a rotating milling device (TASK WP-B8-2.2 ENEA-EURATOM assoc. 1998).
JPBL Series		Pebble (~ $\phi 1$)	These pebbles were fabricated by the wet process with substitution reaction.
JPLT Series		Pellet ($\phi 10 \times 8$)	These pellets were fabricated by the cold pressing and sintering method.

Figure 1 Photographs and shapes of specimens in this study.

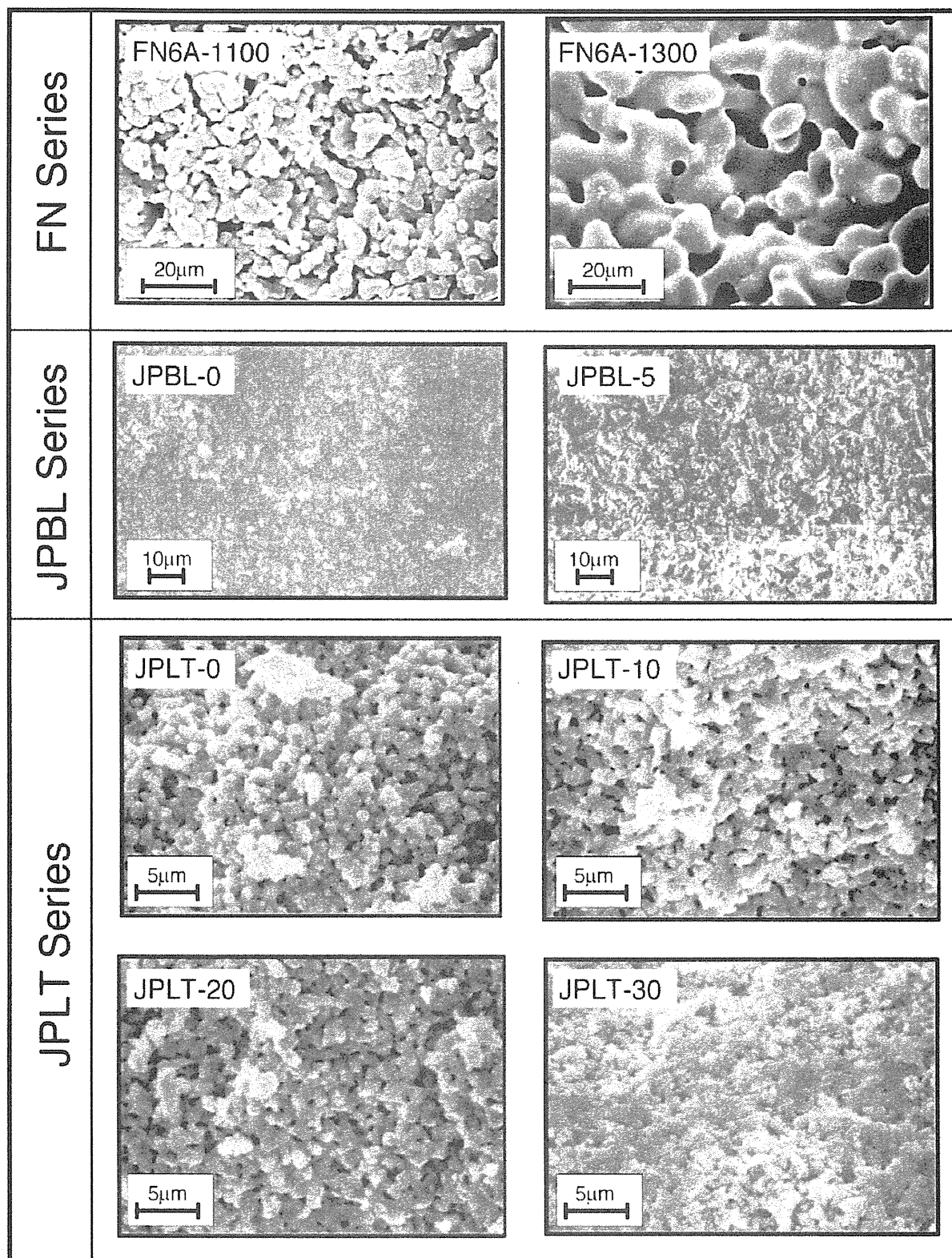


Figure 2 SEM photographs of as received surfaces of main specimens.

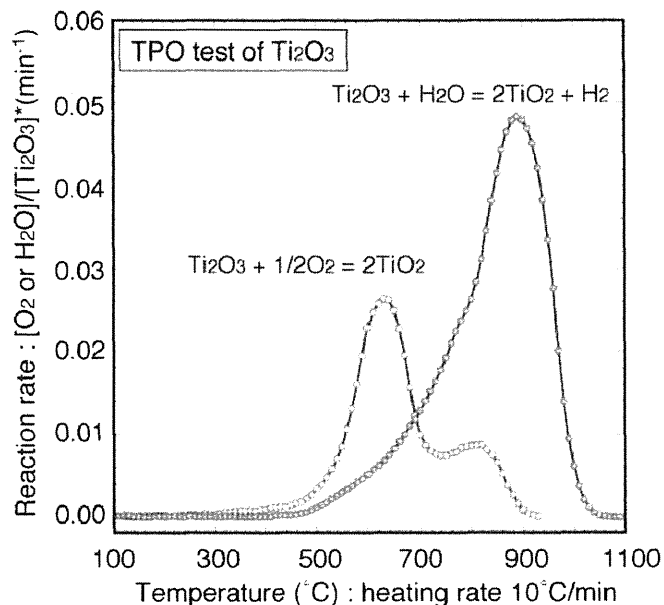


Figure 3 Oxidation rate of Ti_2O_3 powder in $\text{He}+0.1\%\text{O}_2$ ($+\text{O}_2$ in figures) and in $\text{Ar}+1.5\%\text{H}_2\text{O}$ ($+\text{H}_2\text{O}$ in figures) [12].

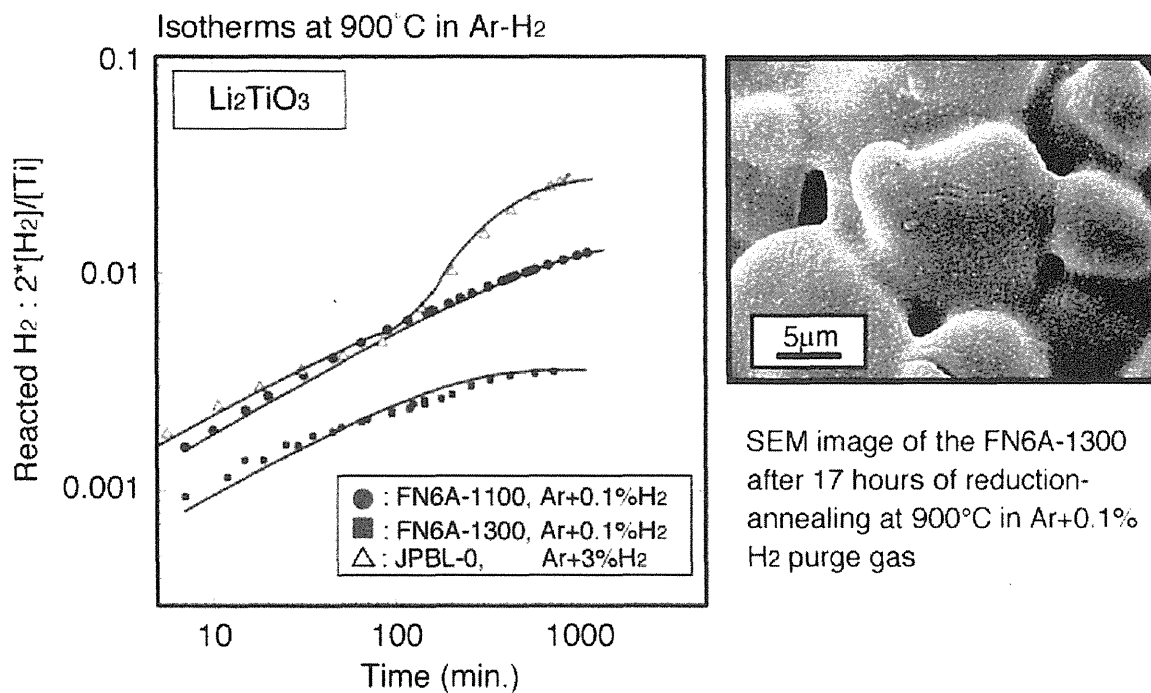


Figure 4 Evolution of $\Delta = 2x$ in $\text{Li}_2\text{TiO}_{3-x}$ during pure Li-metatitanate pebbles (Tables 1 and 3) reduction at 900°C in $0.1\%\text{H}_2$ (black squares) and $3\%\text{H}_2$ (open triangles) Ar doped sweeping gas. The cross points refer to the FN6A-1300 pebbles showing a nucleation of a new phase on the grain surfaces after its reduction.

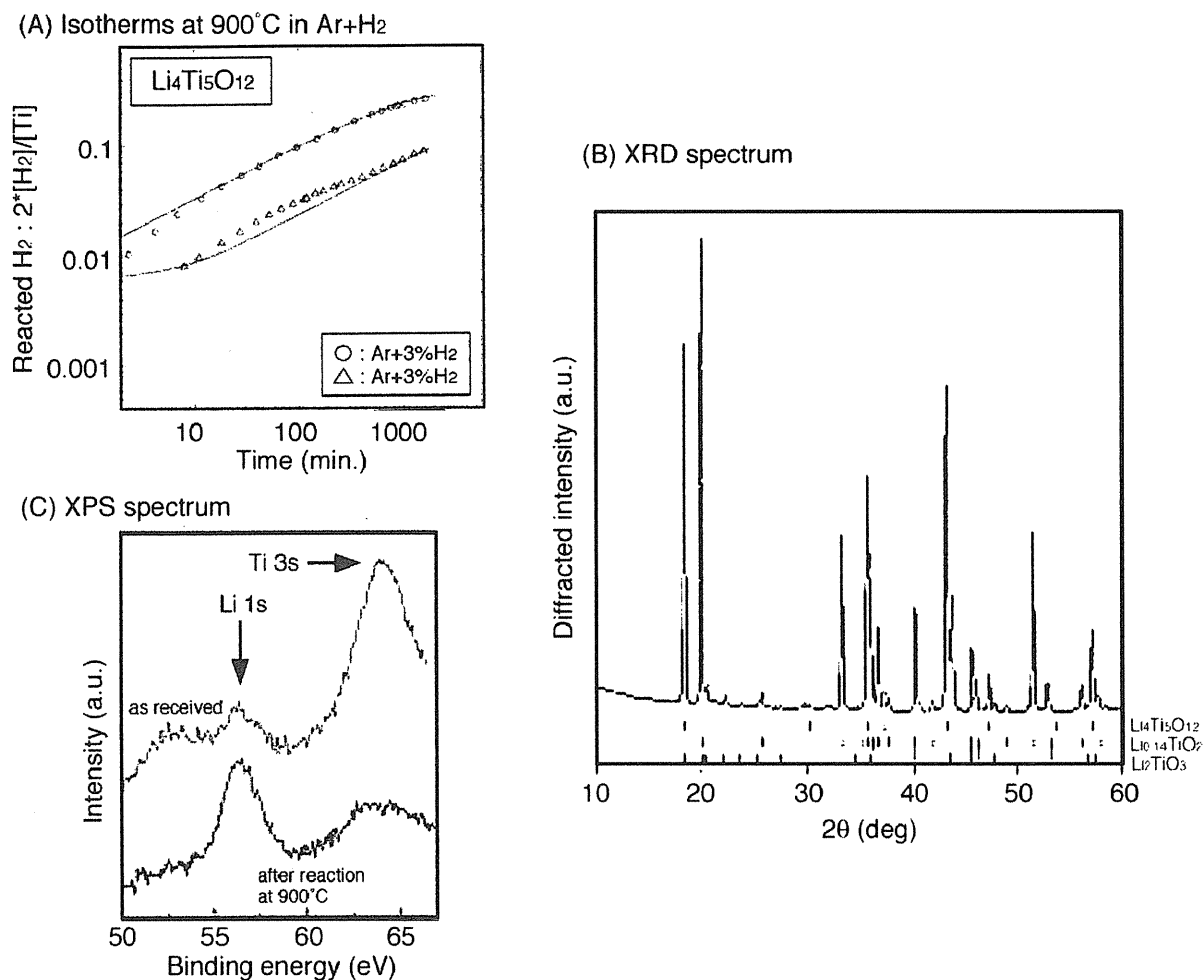


Figure 5 A) Average Δ measured during $\text{Li}_4\text{Ti}_5\text{O}_{12}$ pebbles reduction at 900°C in Ar+3% H_2 (upper data) and in Ar+0.1% H_2 . XRD (B) and XPS (C, lower signal) of the air exposed final product show, respectively, formation of Li_xTiO_2 , mainly orthorhombic $\text{Li}_{0.14}\text{TiO}_2$, and a sharp increase of lithium concentration on the surface. [Compare the Li/Ti peak ratio before (upper signal) and after (lower signal) the reduction.]

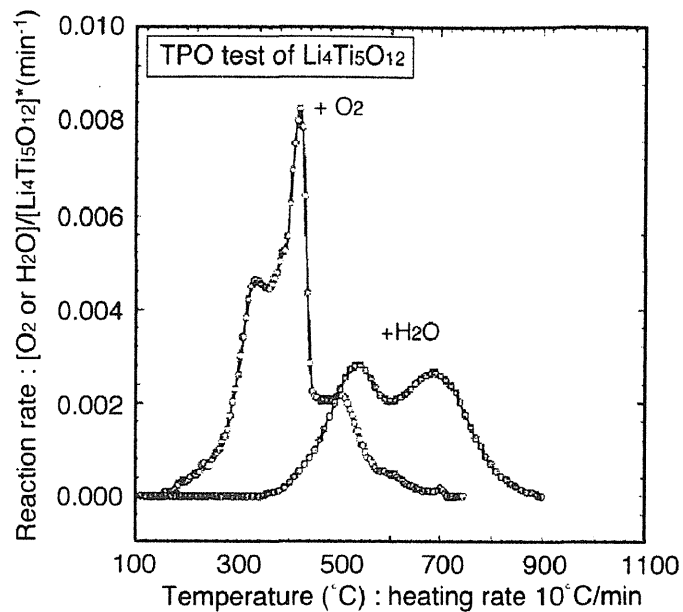


Figure 6 Oxidation rate of the “black” reduced product of spinel powder by TPO (spectra (on the left) obtained using He+0.1%O₂ (+O₂ in figure) and Ar+1.5%H₂O (+H₂O in figure) [12].

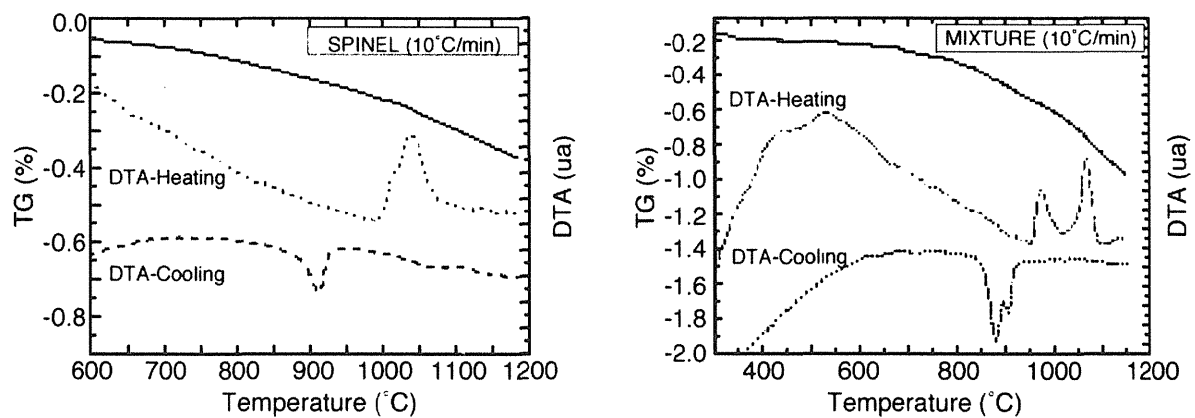


Figure 7 TG and DTA curves for pure Li₄Ti₅O₁₂ spinel powder (left) and its mixture with Li₂TiO₃ (right) under dynamic heating in Ar+3% H₂ atmosphere.

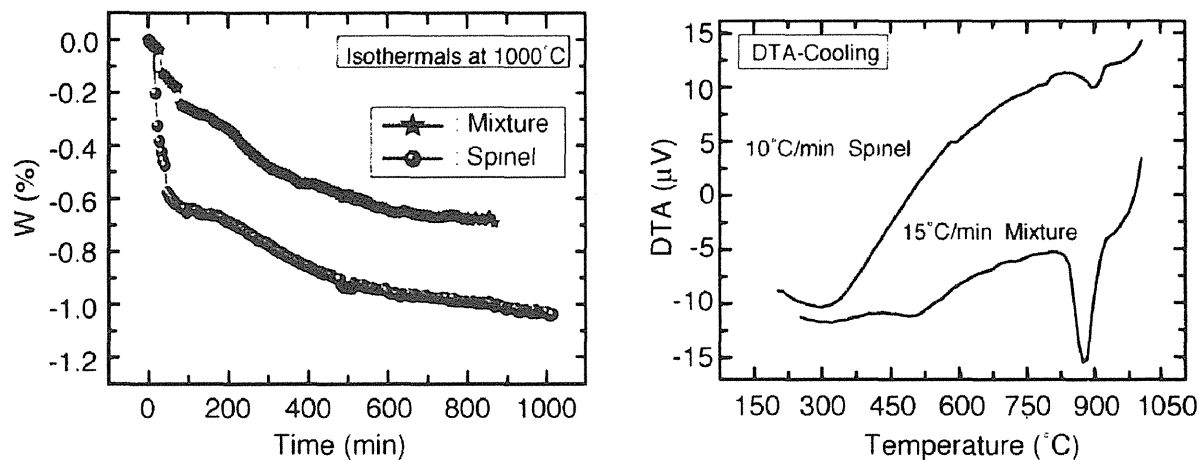


Figure 8 Spinel and Mixture weight loss during reduction-annealing at 1000°C (left). After 17 h during their cooling exo-thermal transitions (right), the DTA signals are not calibrated to the amount of specimen [19].

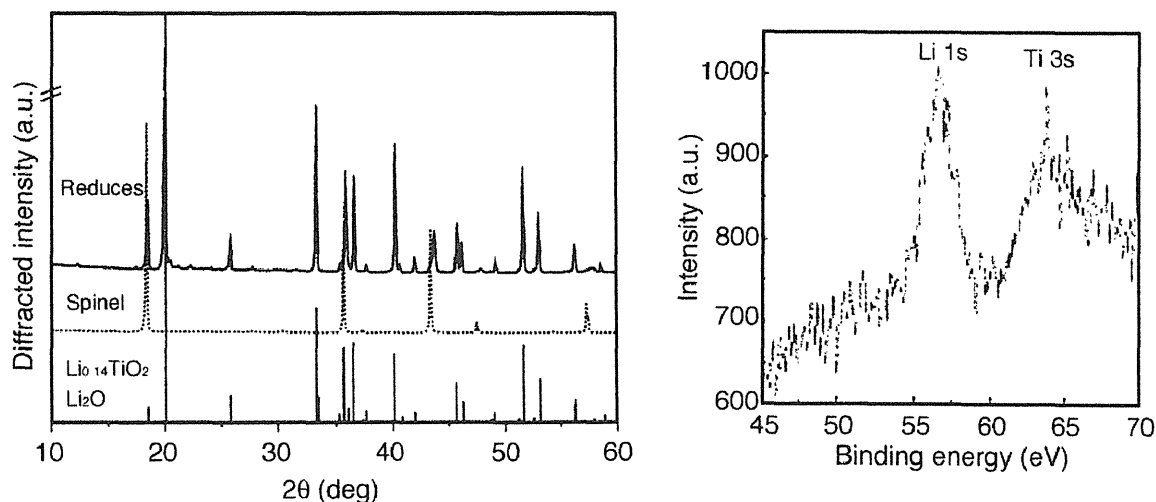


Figure 9 XRD pattern and XPS signal of spinel powder exposed 17 hours at 1000°C to $Ar+3\%H_2$ in the Pt crucible of our TG apparatus [19].

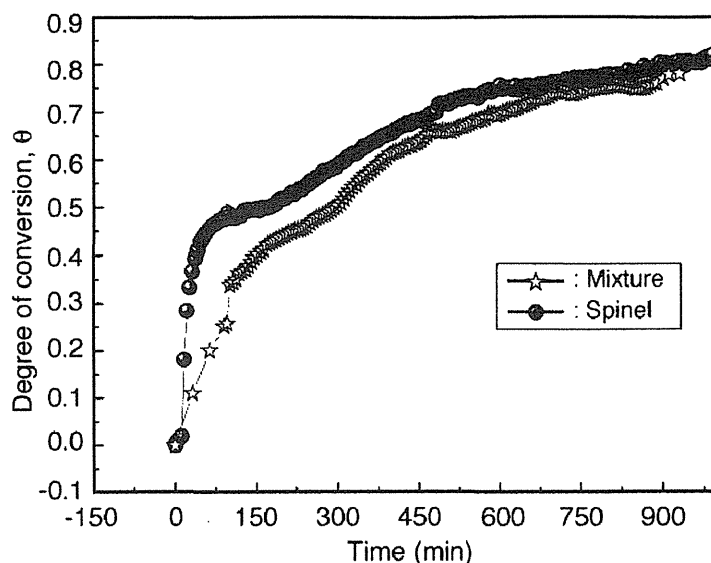


Figure 10 Experimental fractional conversion of the sole spinel phase present in pure spinel and mixture powders as a function of reduction annealing time (in Ar+3% H_2 at 1000°C) [19].

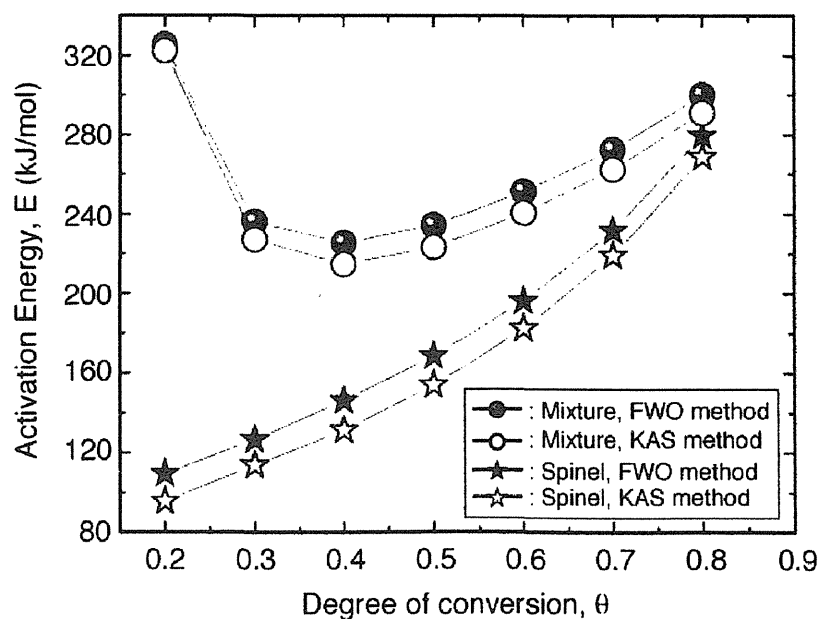


Figure 11 Apparent activation energy for reduction of the spinel and mixture powder specimens reduction in Ar+3% H_2 as a function of the θ extent, degree of conversion. (FWO : Flynn-Wall-Ozawa, KAS : Kissinger-Akahira-Sunose) [19].

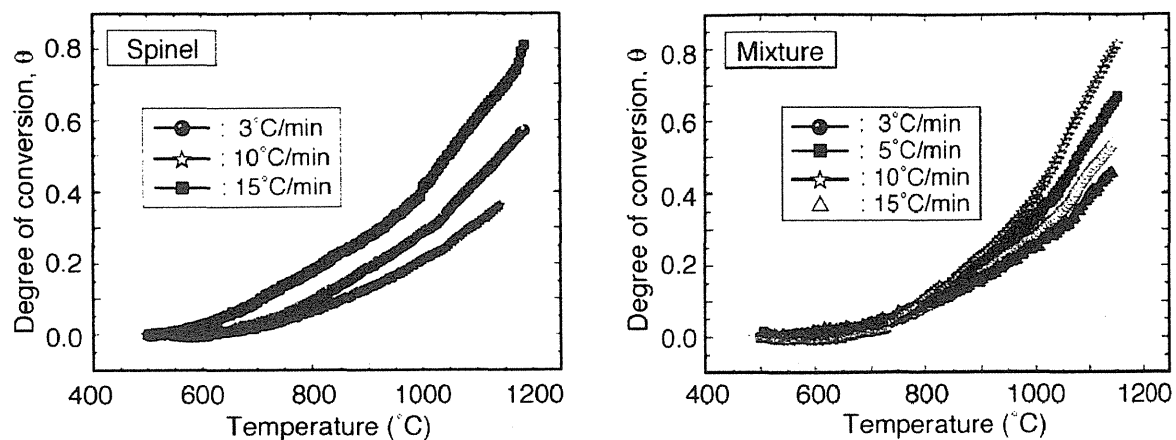


Figure 12 $\theta(T)$ plots obtained for spinel and mixture specimens undergoing heating ramps at various β values [19].

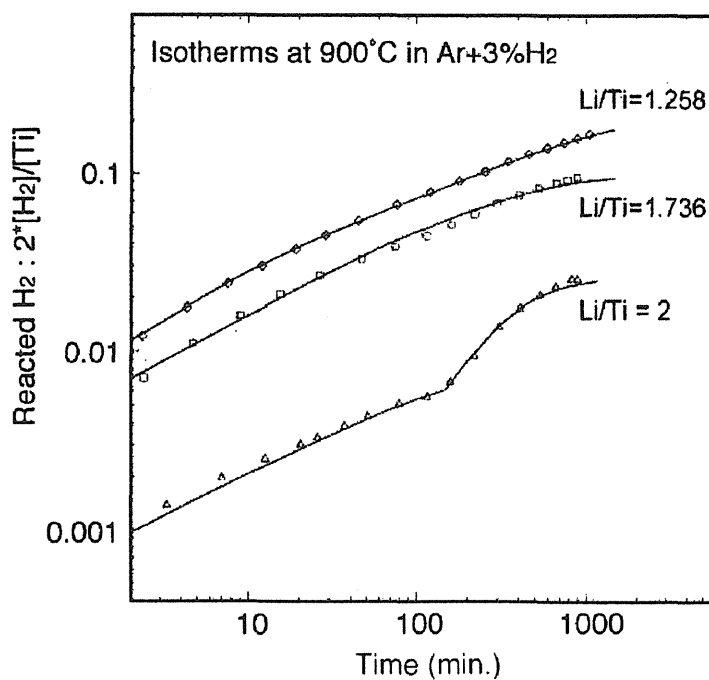
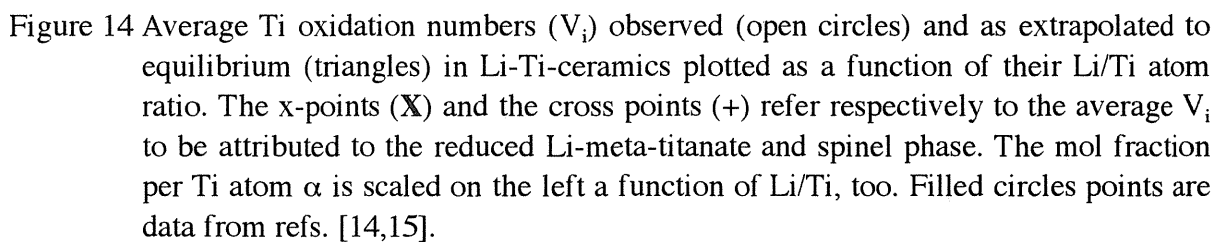


Figure 13 Average Δ evolution in $\text{Ti}^{++\Delta}$ In JPLT-30, JPLT-10 and JPLT-0 specimens (see Table 3) during reduction in $\text{Ar}+3\%\text{H}_2$ at 900°C . See the effect of the 0.17 Li/Ti loss on the reduction rate of the originally stoichiometric ($\text{Li/Ti} = 2$) specimen [20].



Appendix I : Kinetic Elaboration by Thermogravimetric Tests

AI-1. TG isothermal tests: kinetic elaboration.

The experimental $\theta(t)$ curves (Figure 10 in the text) were sectioned in θ fields in which they were compared to the theoretical formula (11) in the text by using the $g(\theta)$ of Table A1. The aim was to individuate the best-fitting mechanism for each zone of θ by the method described in ref. [A-1]. The results are reported in Figures A1 and A2 [A-2] and Table A2.

AI-2. TG dynamic tests: kinetic elaboration.

Equation (12) is a non linear differential equation which is approximated to manageable formulas to get the kinetics parameters, mainly the activation energy E. That is approximated by eqs. (A1) [A-3] or (A2) [A-4] in the isoconversional integral method applied to data obtained by varying β (Figure 13 in the text) [A-5, A-6, A-7].

$$\text{FWO} \quad \ln \beta = \ln \frac{AE}{Rg(\theta)} - 5.331 - 1.052 \frac{E}{RT} \quad (\text{A1})$$

For $\theta = \text{costant}$ the $\ln \beta$ vs $(1/T)$ plots should be a straight line whose slope gives E with an error higher than 10% for $E/RT < 20$.

The second method known as KAS (Kissinger-Akahira-Sunose) [A-4] is based on the Coats-Redfern [A-8] approximation of the eq. (11) in the text. In this case the slope of $\ln(\beta^2/T)$ vs $1/T$ gives E.

$$\text{KAS} \quad \ln \frac{\beta}{T^2} = \ln \frac{AR}{Eg(\theta)} - \frac{E}{RT} \quad (\text{A2})$$

The application of FWO and KAS methods to our results are reported in Figure A3 [A-2].

References

- [A-1] I.A. Leonidov et al., Structure, ionic conduction, and phase transformations in lithium titanate $\text{Li}_4\text{Ti}_5\text{O}_{12}$, Phys. of Solid State 45 (2003) 2183.
- [A-2] M.R. Mancini, V. Contini, K. Tsuchiya, et al., "Thermochemistry of Li-Titanates ceramics in reducing environments," The 23rd Symposium on Fusion Technology (SOFT-23), 2004, Venice, Italy, to be published in Fusion Eng. Des.
- [A-3] H. Sharp, G. Brindley, B.N. Narahari Achar, J. Am. Ceram. Soc. 49 (1966) 379-382.
- [A-4] T. Akakira, T. Sunose, Res. Report Chiba Inst. Technol. (Sci. Technol) 16 (1971) 22.
- [A-5] J.H. Flynn, L.A. Wall, J. res. Nat. Bur. Stand. A. Phys. Chem. 70 (1966) 487.
- [A-6] T. Ozawa, Bull. Chem. Soc. Japan 38 (1965) 18-81.
- [A-7] C. Doyle, J. Appl. Polym. Sci. 6 (1962) 632.
- [A-8] A.W. Coats, J.P. Redfern, Nature 201 (1964) 68.

Table A1 Forms of $f(\theta)$ and $g(\theta)$ for different reaction mechanism

Symbol	Kinetic model	$f(\theta)$	$g(\theta)$
Nucleation and nuclei growth			
A2	Avrami-Erofeev	$2(1-\theta)[- \ln(1-\theta)]^{1/2}$	$[- \ln(1-\theta)]^{-1/2}$
A3		$3(1-\theta)[- \ln(1-\theta)]^{2/3}$	$[- \ln(1-\theta)]^{-1/3}$
A4		$4(1-\theta)[- \ln(1-\theta)]^{3/4}$	$[- \ln(1-\theta)]^{-1/4}$
Phase-boundary reaction			
R2	Two-dimensional movement (shrinking cylinder)	$[2(1-\theta)]^{1/2}$	$[1-(1-\theta)^{1/2}]$
R3	Three-dimensional movement (shrinking sphere)	$[3(1-\theta)]^{2/3}$	$[1-(1-\theta)^{1/3}]$
Diffusion mechanism			
D1	One-dimensional diffusion	$1/(2\theta)$	θ^2
D2	Two-dimensional diffusion	$[- \ln(1-\theta)]^1$	$(1-\theta)\ln(1-\theta)$
D3	Three-dimensional diffusion	$3/2(1-\theta)^{2/3}[1-(1-\theta)]^{1/3}]^1$	$[1-(1-\theta)^{1/3}]^2$
D4	Ginstling-Brounshtein	$3/2[(1-\theta)^{-1/3}-1]^1$	$[1-(2\theta/3)]-(1-\theta)^{2/3}$
A-J	Counter diffusion		$[(1+\theta)]^{1/3}-1]^2$
n-Order reactions			
F1	First order	$(1-\theta)$	$-\ln(1-\theta)$
F2	Second order	$(1-\theta)^2$	$1/[1-\theta]$
F3	Third order	$(1-\theta)^3$	$1/[1-\theta]^2$

Table A2 Rate (K) and time (τ) constants with the related correlation factor (r^2) as evaluated by using the models best-fitting the data in the different ranges of θ for spinel and mixture powders at 1000°C in Ar + 3% H_2

Sample	Models	θ	$K (10^{-2} \text{ h}^{-1})$	$\tau (\text{h})$	r^2
Spinel	A-J	< 0.34	1.93	52	0.998
	D3	0.34 - 0.40	0.014	7342	0.996
	R3	0.40 - 0.60	1.45	69	0.999
	R2	0.60 - 0.72	0.68	147	0.997
Mixture	R2	< 0.34	3.38	29.5	0.994
		0.34 - 0.40	0.018	5555	0.996
	R3	0.41 - 0.54	2.31	43	0.998
		0.54 - 0.70	0.77	130	0.987

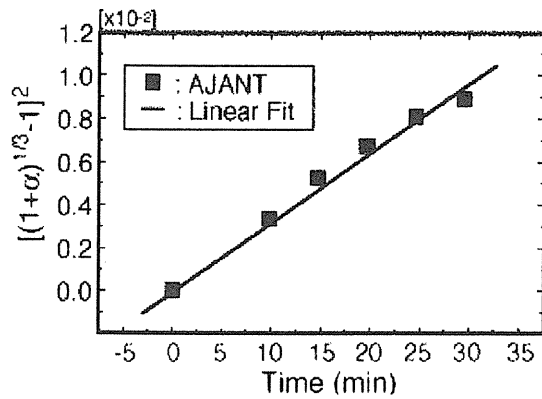
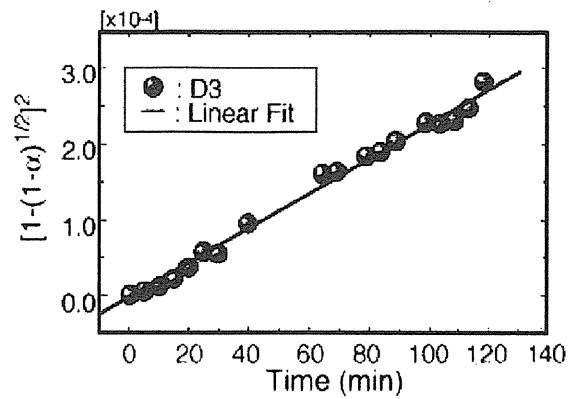
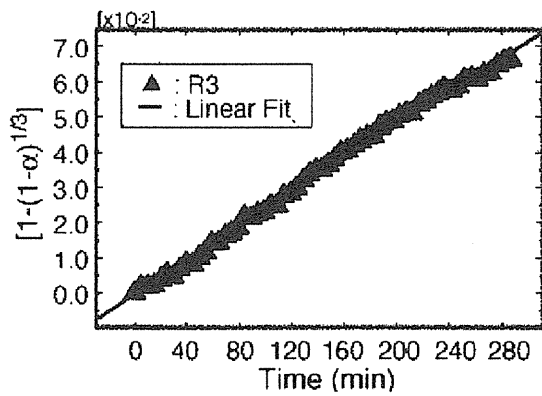
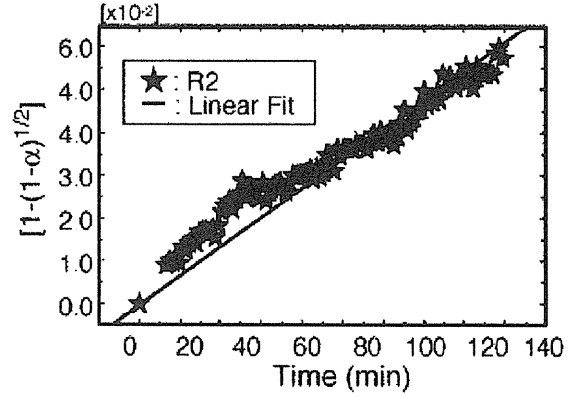
(A) Diffusion mechanism
(Counter diffusion)(B) Diffusion mechanism
(Three-dimensional diffusion)(C) Phase-boundary reaction
(Three-dimensional movement)(D) Phase-boundary reaction
(Two-dimensional movement)

Figure A1 Spinel phase powder reduction. Time plots of the best data fitting to $g(\theta)$ models of Table A1 [A-2].

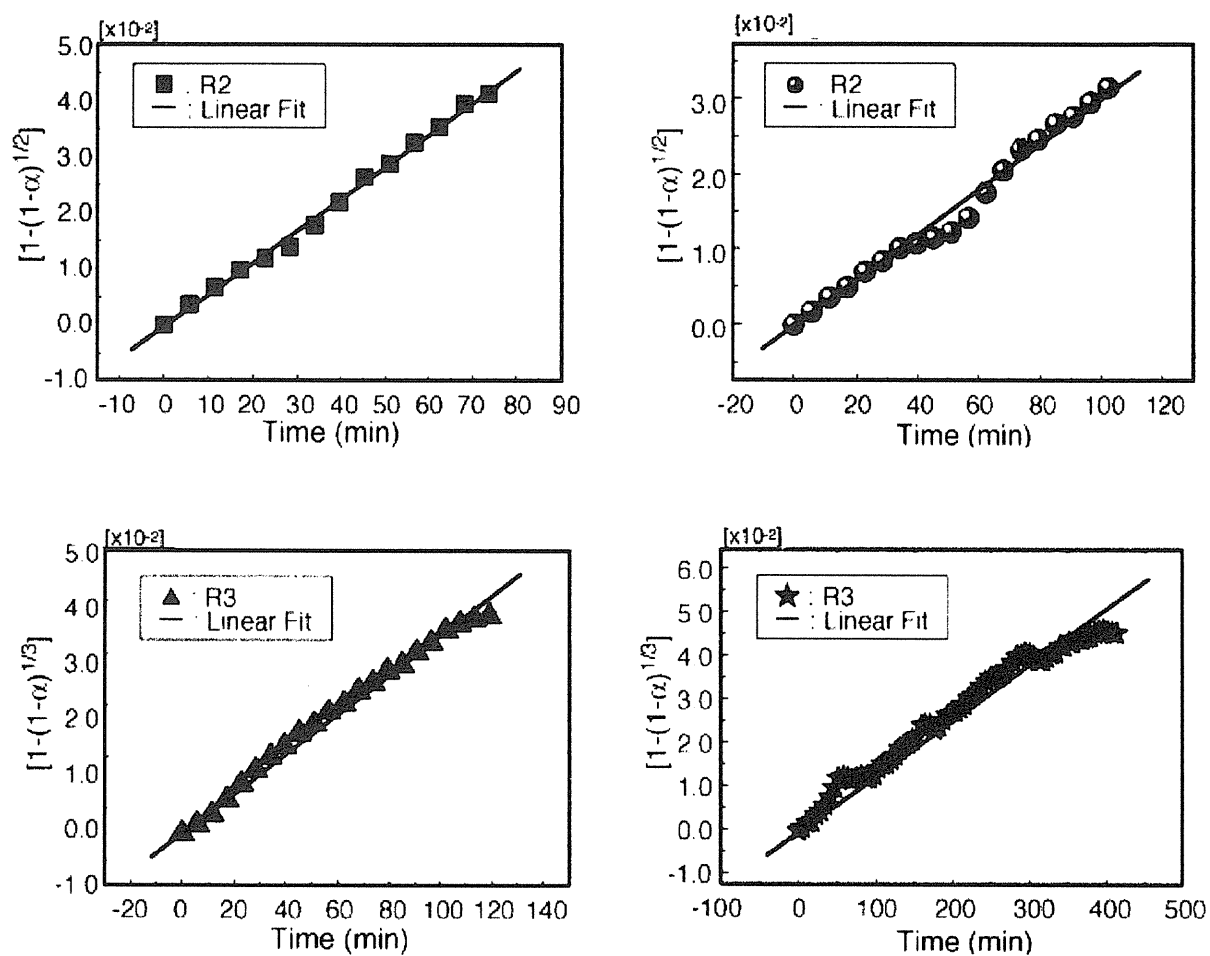


Figure A2 Mixture powder reduction. Time plots of the best data fitting to $g(\theta)$ models of Table A1 [A-2].

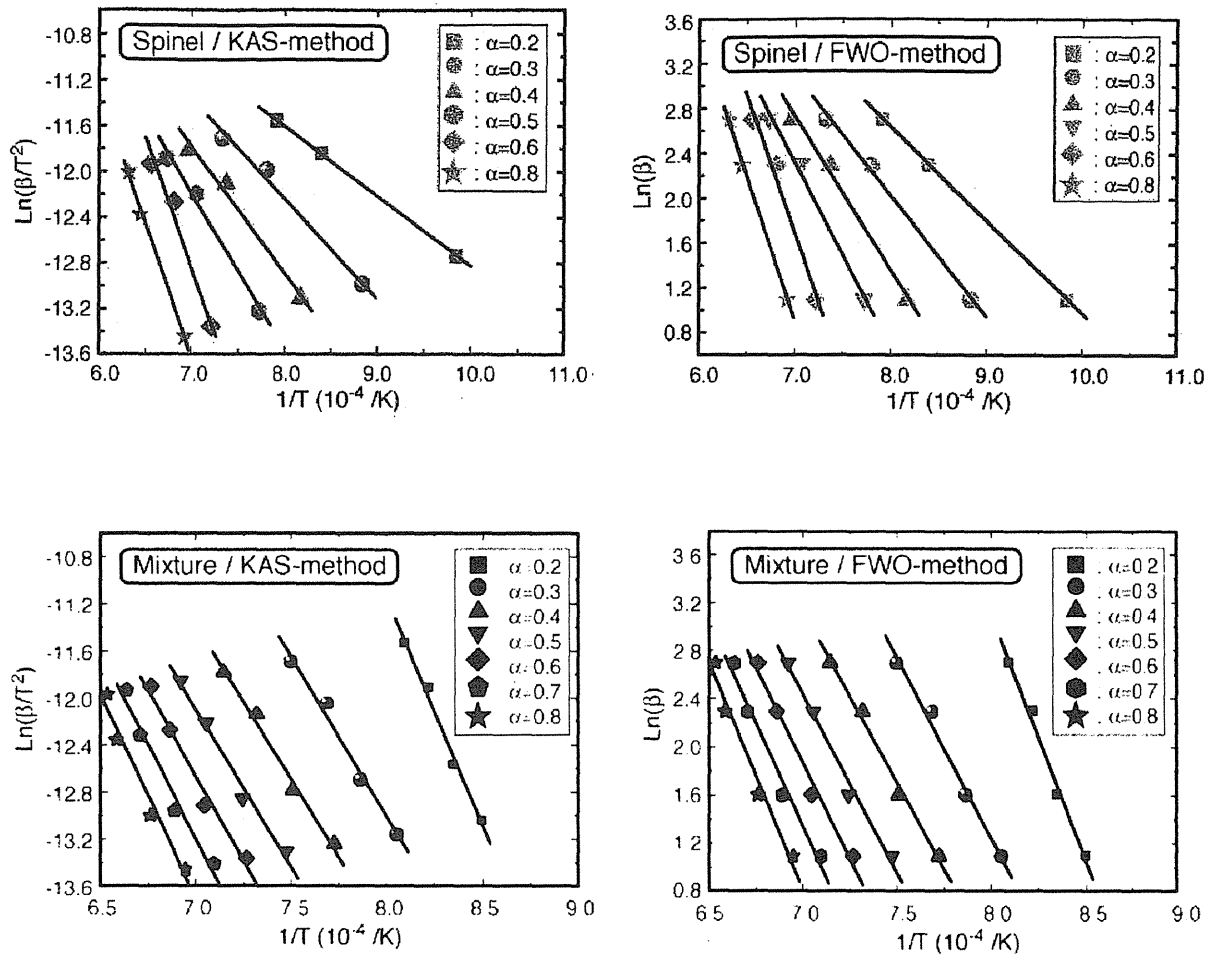


Figure A3 Application of FWO and KAS methods to spinel and mixture powder specimen reductions in $\text{Ar}+3\%\text{H}_2$ [A-2].

Appendix II : Results in This Collaboration

A-II.1 Papers

- 1) K. Tsuchiya, C. Alvani, H. Kawamura, H. Yamada, S. Casadio, V. Contini, “Effect of TiO_2 on the Reduction of Lithium Titanate Induced by H_2 in the Sweep Gas,” The 22nd Symposium on Fusion Technology (SOFT-22) 2002, Helsinki, Finland, Fusion Eng. Des., 69 (2003) 443-447.
- 2) K. Tsuchiya, H. Kawamura, M. Uchida, S. Casadio, C. Alvani, Y. Ito, “Improvement of Sintered Density of Li_2TiO_3 Pebbles Fabricated by Direct-wet Process,” The 22nd Symposium on Fusion Technology (SOFT-22) 2002, Helsinki, Finland, Fusion Eng. Des., 69 (2003) 449-453.
- 3) K. Tsuchiya, H. Kawamura, S. Casadio, C. Alvani, “Effects of gelation and sintering conditions on granulation of Li_2TiO_3 pebbles from Li-Ti complex solution,” The 23rd Symposium on Fusion Technology (SOFT-23), 2004, Venice, Italy, to be published in Fusion Eng. Des.
- 4) C. Alvani, K. Tsuchiya, V. Contini, F. Pierdominici, H. Kawamura, S. Casadio, “Kinetics of Li depleted Li_2TiO_3 reaction with H_2 added to Ar purge gas,” The 23rd Symposium on Fusion Technology (SOFT-23), 2004, Venice, Italy, to be published in Fusion Eng. Des.
- 5) M.R. Mancini, V. Contini, K. Tsuchiya, et al., “Thermochemistry of Li-Titanates ceramics in reducing environments,” The 23rd Symposium on Fusion Technology (SOFT-23), 2004, Venice, Italy, to be published in Fusion Eng. Des.
- 6) C. Alvani, S. Casadio, V. Contini, K. Tsuchiya, H. Kawamura, R. Giorgi and R. Mancini, “Effect of reduction by H_2 and re-oxidation by H_2O splitting of Li-titanates”, to be published in J. Solid State Chem.

A-II.2 Contributions to conferences

- 1) K. Tsuchiya, M. Uchida, H. Kawamura, S. Casadio, C. Alvani, “Fabrication Tests of Li_2TiO_3 Pebbles by Direct Wet Process,” Proc. of the 10th International Workshop on Ceramic Breeder Blanket Interactions (CBBI-10), (FZKA 6720), (2002) pp93-100.
- 2) C. Alvani, S. Casadio, V. Contini, R. Giorgi, M.R. Mancini, K. Tsuchiya, H. Kawamura, et al., “High temperature reactivity of Li-titanates with H_2 contained in purge gas,” Proc. of the 11th International Workshop on Ceramic Breeder Blanket Interactions (CBBI-11), JAERI-Conf 2004-012, (2004).
- 3) C. Alvani, S. Casadio, V. Contini, R. Giorgi, R. Mancini, K. Tsuchiya, H. Kawamura, “Lithium depletion vs. Oxygen loss correlation for Li_2TiO_3 pebbles as exposed to the HCPB “hot spot” conditions,” The 12th International Workshop on Ceramic Breeder Blanket Interactions (CBBI-12), Karlsruhe, Germany.

A-II.3 Patents

- 1) S. Casadio, C. Alvani, K. Tsuchiya, H. Kawamura, “A process for Recovery of Ceramic Lithium Metatitanate,” Patent in Italy (BO2004A000428) and Japan (JP2004-266813), 2004.

A-II.4 Cooperation experiments

- 1) K. Tsuchiya : Mar. 4, 2002 to Mar. 14, 2002., in C. R. Cassasia, ENEA
- 2) K. Tsuchiya : Feb. 16, 2004 to Feb. 25, 2004., in C. R. Cassasia, ENEA

国際単位系 (SI) と換算表

表 1 SI 基本単位および補助単位

量	名 称	記 号
長 さ	メ ー ト ル	m
質 量	キ ロ グ ラ ム	kg
時 間	秒	s
電 流	ア ン ペ ア	A
熱力学温度	ケ ル ビ ン	K
物 質 量	モ ル	mol
光 度	カ ン デ ラ	cd
平 面 角	ラ ジ ア ン	rad
立 体 角	ステラジアン	sr

表 3 固有の名称をもつ SI 組立単位

量	名 称	記号	他の SI 単位 による表現
周 波 数	ヘ ル ツ	Hz	s ⁻¹
力	ニ ユ ー ト ン	N	m·kg/s ²
圧 力 , 応 力	パ ス カ ル	Pa	N/m ²
エネルギー, 仕事, 熱量	ジ ュ ー ル	J	N·m
工 率 , 放 射 束	ワ ッ ト	W	J/s
電 気 量 , 電 荷	ク ー ロ ン	C	A·s
電位, 電圧, 起電力	ボ ル ト	V	W/A
静 電 容 量	フ ァ ラ ド	F	C/V
電 気 抵 抗	オ ー ム	Ω	V/A
コンダクタンス	ジ ー メ ン ス	S	A/V
磁 束	ウ ェ ー バ	Wb	V·s
磁 束 密 度	テ ス ラ	T	Wb/m ²
インダクタンス	ヘ ン リ ー	H	Wb/A
セルシウス温度	セルシウス度	°C	
光 束 度	ル ー メ ン	lm	cd·sr
照 射 度	ル ク ス	lx	lm/m ²
放 射 能	ベ ク レ ル	Bq	s ⁻¹
吸 収 線 量	グ レ イ	Gy	J/kg
線 量 当 量	シーベルト	Sv	J/kg

表 2 SI と併用される単位

名 称	記 号
分, 時, 日	min, h, d
度, 分, 秒	°, ', "
リットル	l, L
トン	t
電子ボルト	eV
原子質量単位	u

1 eV=1.60218×10⁻¹⁹ J

1 u=1.66054×10⁻²⁷ kg

表 4 SI と共に暫定的に
維持される単位

名 称	記 号
オングストローム	Å
バ ー ン	b
バ ー ル	bar
ガ ル	Gal
キ ュ リ ー	Ci
レ ン ト ゲ ン	R
ラ ド	rad
レ ム	rem

1 Å=0.1 nm=10⁻¹⁰ m

1 b=100 fm²=10⁻²⁸ m²

1 bar=0.1 MPa=10⁵ Pa

1 Gal=1 cm/s²=10⁻² m/s²

1 Ci=3.7×10¹⁰ Bq

1 R=2.58×10⁻⁴ C/kg

1 rad=1 cGy=10⁻² Gy

1 rem=1 cSv=10⁻² Sv

表 5 SI 接頭語

倍数	接頭語	記 号
10 ¹⁸	エクサ	E
10 ¹⁵	ペタ	P
10 ¹²	テラ	T
10 ⁹	ギガ	G
10 ⁶	メガ	M
10 ³	キロ	k
10 ²	ヘクト	h
10 ¹	デカ	da
10 ⁻¹	デシ	d
10 ⁻²	センチ	c
10 ⁻³	ミリ	m
10 ⁻⁶	マイクロ	μ
10 ⁻⁹	ナノ	n
10 ⁻¹²	ピコ	p
10 ⁻¹⁵	フェムト	f
10 ⁻¹⁸	アト	a

(注)

- 表 1～5 は「国際単位系」第 5 版, 国際度量衡局 1985 年刊行による。ただし, 1 eV および 1 u の値は CODATA の 1986 年推奨値によった。
- 表 4 には海里, ノット, アール, ヘクトールも含まれているが日常の単位なのでここでは省略した。
- bar は, JIS では流体の圧力を表わす場合に限り表 2 のカテゴリーに分類されている。
- EC 閣僚理事会指令では bar, barn および「血圧の単位」mmHg を表 2 のカテゴリーに入れている。

換 算 表

力	N(=10 ⁵ dyn)	kgf	lbf
	1	0.101972	0.224809
	9.80665	1	2.20462
	4.44822	0.453592	1

粘 度 1 Pa·s(N·s/m²)=10 P(ポアズ)(g/(cm·s))

動粘度 1 m²/s=10⁴ St(ストークス)(cm²/s)

圧	MPa(=10 bar)	kgf/cm ²	atm	mmHg(Torr)	lbf/in ² (psi)
	1	10.1972	9.86923	7.50062×10 ³	145.038
力	0.0980665	1	0.967841	735.559	14.2233
	0.101325	1.03323	1	760	14.6959
	1.33322×10 ⁻⁴	1.35951×10 ⁻³	1.31579×10 ⁻³	1	1.93368×10 ⁻²
	6.89476×10 ⁻³	7.03070×10 ⁻²	6.80460×10 ⁻²	51.7149	1

エネルギー・仕事・熱量	J(=10 ⁷ erg)	kgf·m	kW·h	cal(計量法)	Btu	ft·lbf	eV
	1	0.101972	2.77778×10 ⁻⁷	0.238889	9.47813×10 ⁻⁴	0.737562	6.24150×10 ¹⁸
	9.80665	1	2.72407×10 ⁻⁶	2.34270	9.29487×10 ⁻³	7.23301	6.12082×10 ¹⁹
	3.6×10 ⁶	3.67098×10 ⁵	1	8.59999×10 ⁵	3412.13	2.65522×10 ⁶	2.24694×10 ²⁵
	4.18605	0.426858	1.16279×10 ⁻⁶	1	3.96759×10 ⁻³	3.08747	2.61272×10 ¹⁹
	1055.06	107.586	2.93072×10 ⁻⁴	252.042	1	778.172	6.58515×10 ²¹
	1.35582	0.138255	3.76616×10 ⁻⁷	0.323890	1.28506×10 ⁻³	1	8.46233×10 ¹⁸
	1.60218×10 ⁻¹⁹	1.63377×10 ⁻²⁰	4.45050×10 ⁻²⁶	3.82743×10 ⁻²⁰	1.51857×10 ⁻²²	1.18171×10 ⁻¹⁹	1

1 cal = 4.18605 J (計量法)

= 4.184 J (熱化学)

= 4.1855 J (15 °C)

= 4.1868 J (国際蒸気表)

仕事率 1 PS (仏馬力)

= 75 kgf·m/s

= 735.499 W

放射能	Bq	Ci
	1	2.70270×10 ⁻¹¹
	3.7×10 ¹⁰	1

吸収線量	Gy	rad
	1	100
	0.01	1

照射線量	C/kg	R
	1	3876
	2.58×10 ⁻⁴	1

線量当量	Sv	rem
	1	100
	0.01	1

(86 年 12 月 26 日現在)

Li Depletion Effects on Li_2TiO_3 Reaction with H_2 in Thermo-chemical Environment Relevant to Breeding Blanket for Fusion Power Plants



古紙配合率 100%
白色度 70% 再生紙を使用しています